Review

Biochar Derived from Agricultural Residues for Wastewater Contaminants Removal

Pengyun Liu , Luisa Boffa , Giancarlo Cravotto *

Posted Date: 4 December 2025

doi: 10.20944/preprints202512.0318.v1

Keywords: environmental remediation; circular economy; biochar utilization; agriculture residue valorization; adsorption decontaminant and recovery

 doi:10.20944/preprints202512.0318.v1

Review

Biochar Derived from Agricultural Residues for Wastewater Contaminants Removal

Pengyun Liu, Luisa Boffa and Giancarlo Cravotto *

Department of Drug Science and Technology, University of Turin, via P. Giuria 9, 10125 Turin, Italy

* Correspondence: giancarlo.cravotto@unito.it; Tel: +39.011.670.7183; Fax: +39.011.670.7162.

Abstract

The valorization of agricultural residues helps improve crop economic efficiency and alleviate environmental pressures. Owing to the merits of simplicity, high efficiency, low costs, and scalability, adsorption removal of contaminants using biochar has been widely investigated. The adsorption removal of organic and inorganic contaminants from wastewater using biochar derived from agricultural residue follows the principles of the circular economy and green chemistry, facilitating both environmental remediation and agricultural development. This review outlined the mechanism of biochar adsorption, the preparation of biochar from agricultural residues, and their applications for wastewater remediation. Furthermore, the economic evaluation and environmental impacts, as well as the future directions and challenges, in this field, have also been presented.

Keywords: environmental remediation; circular economy; biochar utilization; agriculture residue valorization; adsorption decontaminant and recovery

1. Introduction

Wastewater from various industries poses a tremendous environmental problem and health risk to human beings and water ecosystems [1]. Abundant agricultural wastes are continuously produced globally. It has been reported that the dry biomass production is over 200 billion tons per year around the world, causing a huge agricultural burden [2]. The remediation of wastewater and the appropriate disposal of these agricultural wastes are of great significance to mitigate the aforementioned burden and address these issues.

Adsorption has been a widely applied physicochemical strategy for wastewater purification and the recovery of useful compounds from wastewater [3], owing to the various well-known merits, such as high cost-efficiency, simple design and implementation, high efficiency, robustness, effectiveness, scalability, and sustainability, technically flexible, technologically feasible, and environmentally friendly, free of by-products, simultaneous removal of various contaminants, and resilience against toxic contaminants [4–6]. On the other hand, the limitations of adsorption include the potential for secondary pollution, the production of solid waste, and the requirement for additional treatment to degrade the adsorbed contaminants, among others [7–10]. Appropriate adsorbents are crucial to ensure excellent adsorption performance [3]. Currently, different adsorbents have been fabricated, such as biochar, activated carbon, zeolites, 2-dimensional materials (*e.g.*, graphene, carbon nanotubes, and MXene), resin, bentonite, covalent-organic frameworks, metal-organic frameworks, and composites, among others.[2,11,12]. Among them, carbon materials have attracted increasing attention in recent decades due to their abundant precursors and excellent physicochemical properties, such as numerous surface functional groups, high mechanical strength, and outstanding adsorption performance and reproducibility. As a type of carbon material, biochar is relatively simple and economical to produce and has been widely used for wastewater remediation. The main advantages of biochar compared to other advanced carbon materials, such as activated carbon, carbon nanotubes, and graphene oxide, include its high sustainability (*e.g.*, waste-to-resource principles and renewable feedstock), low energy requirements and production costs, excellent

 doi:10.20944/preprints202512.0318.v1

scalability, and environmental co-benefits (*e.g.*, large-scale applications in agriculture and carbon sequestration, as well as better compatibility with other materials) [7,13–18]. Agricultural wastes have abundant biomass (*e.g.*, lignin, hemicellulose, and cellulose), which is accessible and affordable, and can provide sufficient carbon sources, and thus can be used as green and non-toxic precursor sources of biochar. The preparation of biochar using agricultural wastes not only facilitates the valorization of these wastes but also reduces the environmental and economic burden associated with them (*e.g.*, greenhouse gas emissions). Up to now, biochar has been prepared from date seeds [4], almond shells [19], coconut shells [5,20,21], wheat straw [22], rice husks [21,23–26], corn wastes [27–31], wood wastes [11,32], and rape stalk [33]. The agricultural waste-derived biochar adsorption decontamination is a sustainable and feasible alternative to wastewater remediation [34,35].

Unlike activated carbons, pristine biochar usually possesses a lower surface area and total pore volume, and limited adsorption sites due to poor porosity [14–16,36], followed by poor adsorption ability [37]. Accordingly, the dominant drawbacks of pristine biochar are poor dispersibility (*e.g.*, easy to float and aggregate) [38]. Fortunately, the physicochemical properties (*e.g.*, dispersibility, porosity, separability, mechanical strength, surface area, ionic radius, surface area, electronegativity, and the surface's functional groups, pore size, functional groups, interaction forces, *etc.*) and the adsorption properties (*e.g.*, adsorption capacity, affinity, selectivity), adsorption kinetics, isotherm, and thermodynamics) of a specific biochar can be promoted via activation and modification to improve the porosity, adsorption sites, and surface chemical affinity and interactions [5]. The pristine biochar has been activated using strong acids, strong bases, and metal oxides, and functionalized using various modifiers, via element doping (*e.g.*, N, S, and heavy metals), and surface charge change to better catch target contaminants from wastewater [15,16,22,39–43]. It is worth mentioning that the activation, modification, and functional may reduce the cost-effectiveness of biochar preparation.

Herein, based on the background above, this review presents the recent advances of agricultural waste-derived biochar for wastewater remediation via liquid-solid adsorption, mainly focusing on the adsorption mechanisms, biochar preparation and modification, the main outcomes, the economic evaluation, and environmental impacts. Moreover, the future direction and research needs are also recommended to guide and inspire the incoming work. This review follows the principle of the circular economy and waste valorization, providing a deep understanding of agricultural waste disposal and use, presenting the practical application of wastewater decontamination, and contributing to the sustainable development of agriculture and society globally, as well as resource integration and utilization locally.

2. Mechanism of Adsorption Using Agricultural Residue-Based Biochar

2.1. General Conceptions of Adsorption

Adsorption refers to the process of the transfer of substrates from liquid matrices to the surface and the subsequent inner porous structure of solid adsorbents through the capillary effect [5,27,44]. The adsorption of contaminants from liquids can occur through the adsorption of individual contaminants (*e.g.*, single solute solution), selective adsorption of target compounds in complex matrices, competitive adsorption between several compounds (*e.g.*, naphthalene and phenanthrene in aqueous solution), and simultaneous adsorption of multiple contaminants (*e.g.*, ammonium-N and nitrate-N in wastewater) [30,45,46]. Generally, both chemical and physical adsorption appear during adsorption, but with different contributions. Chemisorption relates to the precursor and chemical composition of biochar (*e.g.*, the type and amounts of surface functional groups (*e.g.*, –OH, C=O, and –COOH), the element components), but physisorption depends on the biochar's surfaces and architecture, and weak interaction forces (*e.g.*, Van der Waals forces) [21]. Thus, the chemisorption is usually a single layer and stronger, in which the adsorbed molecules or ions are difficult to escape from the adsorption site. In contrast, the physisorption is commonly multiple adsorptions and relevant weak, thus, allowing the mitigation of the adsorbed compounds into the inner pores [14,15,45,47]. The performance and properties of adsorption decontamination from wastewater

 doi:10.20944/preprints202512.0318.v1

depends on the physicochemical properties of biochar (*e.g.*, ash content, hydrophobicity, porous property (micro- or meso- porous), point of zero charge (pH_{pzc}), elements composites (*e.g.*, C/O and C/H ratios), and the surface chemical functional groups), the properties of substrates (*e.g.*, pK_a value, solubility, hydrophobicity, chargeability, electron distribution, and molecular or ion size), the interaction between the components in the bulk liquid and the surface of biochar, and so forth [14–16,36,40,45]. The specific absorption may be the synergistic result of these as-mentioned impacts.

2.2. Interactions Between Biochar and Contaminants in Wastewater

Wastewater contains a complex mixture of compounds with a wide range of molecular sizes. Effective adsorption requires that these compounds access the micropores of biochar. Larger molecules are often preferentially adsorbed over smaller ones; however, they can block micropores and hinder the diffusion of smaller molecules into narrower pores. Particle size of the biochar, such as powder versus granular, influences adsorption kinetics by limiting intraparticle mass transfer, but does not change the overall adsorption capacity, which depends on the total specific surface area of the biochar [39]. Biochar with a high surface area and an abundant porous structure, including mesopores and micropores, provides ample adsorption sites for physicochemical interactions with wastewater contaminants [14,15,45,47]. Adsorbent affinity is a key determinant of capacity, irrespective of contaminant concentration [46]. For example, smaller ions typically show higher affinity for reactive sites and are removed more rapidly, yielding superior adsorption performance [49]. In addition, functional groups can contribute substantially when the biochar has a low specific surface area [48]. The dominant physicochemical interactions governing adsorption are critical for contaminant removal and are summarised in Table 1 [2,4,40,50,51]. In particular, hydrophobic compounds are generally adsorbed more readily via hydrophobic interactions than hydrophilic compounds [44]. Groups -OH and $-NH_2$ on the biochar surface are reported to be the dominant groups responsible for the adsorption of anionic dye [48]. The π-π interaction and O-containing groups (*e.g.*, -OH and C=O) on the surface of biochar composites could favor the adsorption of cations through the surface polarization and electrostatic attraction [49,50]. Negatively charged biochar can adsorb ammonium ions via electrostatic attraction and H-bonding between O-containing groups, -OH, C–O, –COOH, and –COC– of biochar and ammonium ions, and phosphate via surface precipitation from urine [26,27,51]. Cations Mg^{2+} and Ca^{2+} in biochar can trap PO_4^{3-} and $H_2PO_4^-$ in liquids via precipitation, while anion Cl- of biochar favors adsorbing PO_4^{3-} via electrostatic forces [27,52,53]. The specific interactions that SiO_2 in biochar can enhance the affinity towards PO_4^{3-} via electrostatic interactions and H-bonding (or ligand exchange) by its -OH group, especially at acid pH [26]. Groups like -OH, -COOH, -Ar, Ar-NH_2 (aromatic amines), R1-CO-N-R2R3 (amides), and -$C_5H_{10}N$- (pyridine) of biochar favor the adsorption of ammonium, nitrate, and phosphate through ion exchange [20]. Biochar can interact with both ammonium- and nitrate-N via electrostatic attraction, ion exchange, and physisorption, and the electrostatic attraction is particularly significant [46]. Additionally, positively charged biochar surfaces can also interact with cationic compounds via Coulombic interactions under acidic conditions [54]. The dominant interactions that contributed to the adsorption can be identified via a combined analysis of various adsorption properties and the characterization of biochar before and after adsorption [6,27,55–57].

Table 1. The mechanisms of the adsorption using agricultural residue-based biochar.

Mechanisms	Illustrations	Examples	Refs.
Precipitation	Contaminants can chemically precipitate via reaction with the liquid solute or biochar surface, and are finally adsorbed on the biochar surface	i) Between Al^{3+}, Fe^{3+}, Ca^{2+}, Mg^{2+}, Zn^{2+}, Cu^{2+}, Pb^{2+}, or Cd^{2+} and OH^- at alkaline conditions ii) Between PO_4^{3-} and Fe-doped biochar to form $Fe_3(PO_4)_2{\cdot}(H_2O)_8$	[37,42,58]
Complexation	Biochar surface's functional groups can act as electron donors or acceptors, interact with metal ions or	i) Between -OH groups and Fe^{2+} ii) Between phosphate and ammonium ion iii) Between –COOH, C=O, or –OH with Cr^{6+} iv) Between OH-, C=O or C–OH with Pb^{2+}	[31,40,54]

 doi:10.20944/preprints202512.0318.v1

	ammonium ions to produce complexes	v) Between -NH_2 and Cu^{2+} or Pb^{2+}	
H-bonding	H-bonding (theoretical bond energies of 4–17 kJ/mol) can be formed via the interaction between the functional groups on the biochar surface (*e.g.*, -NH_2 and -OH) with F-, N-, or O-containing molecules	i) Between -OH and ammonium ion or -NO_2 ii) Between -OH and -OH or -NH_2 iii) Between -COOH and its conjugate acid	[5,46,59]
Electrostatic attraction and repulsion	Electrostatic interaction refers to the formation of ionic bonds between surface-charged biochar and ions or charged molecules. Electrostatic interaction is highly related to the pH of liquids, surface charge of the biochar, and pK_a of the target substrates, which can be limited under high pH	i) Between cationic dye and -COO^- of biochar ii) Between the Si-N of biochar and anionic dyes iii) Between Mn^{2+} and -OH, -COOH, or C=O of biochar iv) Between PO_4^{3-} and nitrate or nitrite of biochar v) Between the same ions on the biochar surface and in liquids	[5,48,60]
π-π electron donor–acceptor interaction	π-π interactions (theoretical bond energies of 4-167 kJ/mol) are weak non-covalent bonds, referring to interactions between groups with π electron systems (*e.g.*, -Ph, -C=C-, C=O, -COOH, -OH, and C-O) of the biochar surface and the target compounds	i) Between -Ph of biochar and the enone structure of tetracycline ii) Between -OH or -COOH of biochar surface and -Ph of phenolic compounds	[2,6,12]
Pore-filling	Pore filling is a physisorption process, referring to the substrate being adsorbed and concentrated on biochar's pore, depending on the properties of biochar (*e.g.*, porosity) and the substrate (*e.g.*, polarity)	i) Extensively occurs during various porous biochar involved adsorption	[42,61]
Ion exchange	Ion exchange refers to the exchange of ions between the biochar surface and the charged substrate in liquid	i) Between the SiO_2 of biochar and ammonium-N ii) Between Ca^{2+}, Na^+, or K^+ of biochar and Hg^{2+} iii) Between -COOH, -OH, or -FeOOH of biochar with Cr^{6+}	[26,31,62]
Ligand exchange	Ligand exchange refers to the original ligand of a coordination compound of biochar being selectively substituted by other ligands in liquids, which is limited at high pH	i) Between -OH of biochar and PO_4^{3-} in liquids ii) Between S- or O- containing groups of biochar with Cd^{2+} in liquids	[30,50,63]
Hydrophobic interaction	Hydrophobic interaction refers to the interaction between aromatized, graphitized layers or the hydrophobically modified surface of biochar and hydrophobic substances	i) Extensively occurs between the hydrophobic surface of biochar and hydrophobic compounds ii) Between oleic acid-modified activated biochar and naphthalene	[40,47]
Redox effects	Redox effects occur between biochar surfaces with oxidation or reduction capabilities and substrates in liquids	i) [Adsorbent]-Fe^{2+} + CrO_4^{2-} + $4OH^-$ + $4H_2O$ → 3 $Fe(OH)_3$ +$Cr(OH)_3$	[38]
Van der Waals forces	Van der Waals forces, a weaker electrostatic interaction than H-bonding, refer to non-directional and unsaturated interactions between the biochar surface and substrates in liquids	i) Between the biochar surface and neutral creatinine, urea, or uric acids	[26]

The adsorption mechanisms of organic and inorganic substances on biochar are compiled in Figure 1.

 doi:10.20944/preprints202512.0318.v1

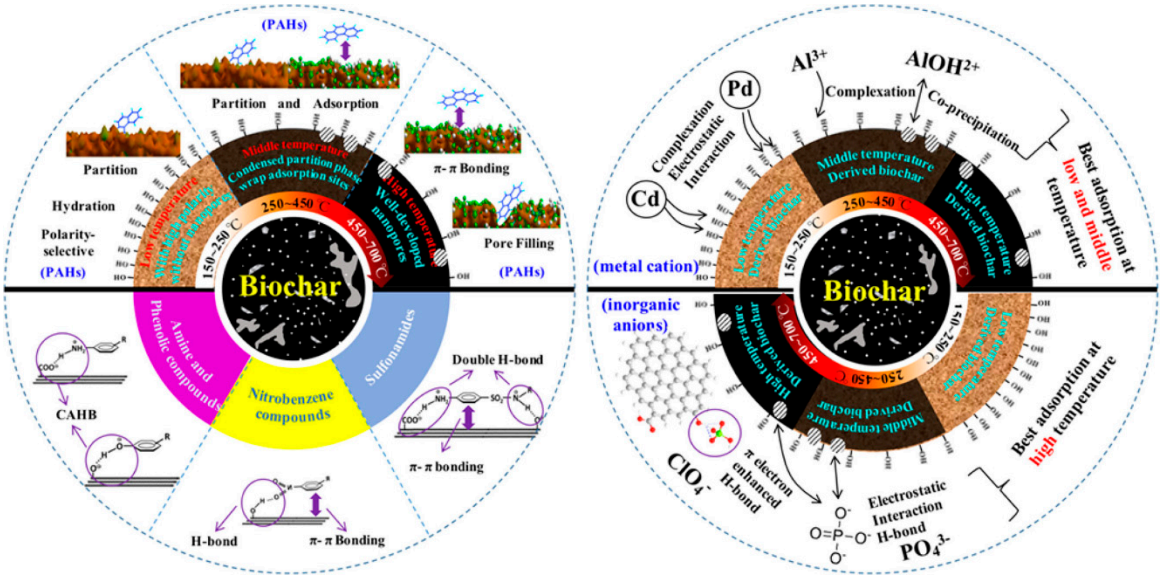

Figure 1. The adsorption mechanisms of organic and inorganic substances on biochar. Reprinted from ref. [64]. Copyright (2018), with permission from ACS.

2.3. Description and Illustration of Adsorption in Wastewater

The static adsorption behaviors and properties can be deconstructed using kinetic, thermodynamic, as well as isotherm models. The kinetic study favors clarifying the rate-control step (*e.g.*, chemical adsorption and mass transfer) during adsorption [4,11]. The most used kinetic models are the pseudo-first order (PFO), the pseudo-second order (PSO), and the Elovich kinetic models [14,65]. In case of high-concentration substances, the PFO model is more suitable to describe the adsorption processes than the PSO model [66]. Adsorption isotherms describe the adsorption layer characteristics and the relationship between the substrates and biochar (*e.g.*, the highest adsorption capacity, physi- or chemi-sorption, and adsorbent surface properties) [14,65]. The frequently applied adsorption isotherm models are the Langmuir, the Freundlich, the Temkin model, the Redlich-Peterson, and the Dubinin-Radushkevich isotherm models [1,2,11,54]. Moreover, Vaishali *et al.* studied the competitive adsorption of methyl paraben, carbamazepine, ibuprofen, and triclosan using Multicomponent Freundlich and Langmuir isotherm models [46]. Adsorption mechanisms (*e.g.*, rate-limiting steps) can commonly be clarified via the Weber and Morris model (also known as the intraparticle diffusion model) and the Boyd model (also known as the film diffusion model) [12]. Moreover, the adsorption thermodynamic properties can be determined using the Arrhenius formula and the Van't Hoff equation with considering the effect of adsorption temperature [11,14,15]. The difficulty of the adsorption can be evaluated using Gibbs free energy (ΔG°), enthalpy (ΔH°), and entropy (ΔS°) [50]. On the other hand, the column adsorption (also known as dynamic adsorption) processes can be described using the Thomas and the Adams–Bohart breakthrough curve models. The higher the column height and the lower the flow rates, the more adsorption sites and the sufficient the axial diffusion and mass transfer, followed by the longer the breakthrough time [50,63].

The equations and their relevant characterizations for describing individual and competitive adsorption capacities of biochar and various models are compiled in Table 2. The applicability, merits, and limitations of these models in adsorption have been well detailed [67–71]. It is worth noting that these models can only speculate on the adsorption mechanism, which should be verified and analysed in combination with practical adsorption investigations and biochar characterizations.

 doi:10.20944/preprints202512.0318.v1

Table 2. The models and equations in biochar adsorption.

Models and equations		Nomenclature	Illustrations	Refs.
Individual adsorption capacity	$q_e=\frac{(C_0-C_e)V}{m}$	C_0- the initial concentration of substrate C_e (mg/L)- the equilibrium concentration q_e (mg/g)- the equilibrium adsorption amount V (L)- the reaction volume m (g)- the biochar's mass	Used for calculating the adsorption capacity of a single substrate	[72]
Competitive adsorption capacity	$C_A=\frac{k_{B\text{-}2}d_{\lambda_A}-k_{B\text{-}1}d_{\lambda_B}}{k_{A\text{-}1}k_{B\text{-}2}-k_{A\text{-}2}k_{B\text{-}1}}$ $C_B=\frac{k_{A\text{-}1}d_{\lambda_B}-k_{A\text{-}2}d_{\lambda_A}}{k_{A\text{-}1}k_{B\text{-}2}-k_{A\text{-}2}k_{B\text{-}1}}$	C_A and C_B (mg·L^{-1})- the concentrations of A and B, respectively $k_{A\text{-}1}$, $k_{A\text{-}2}$, $k_{B\text{-}1}$, and $k_{B\text{-}2}$- the calibration constants for the A and B at their characteristic sorption wavelength (*i.e.*, λ_1 and λ_2) d_{λ_A} and d_{λ_B}- the optical densities of λ_1 and λ_2, respectively	Used for calculating the adsorption capacities of multiple substances	[45]
PFO kinetic model	$\ln\left(q_e-q_t\right)=\ln q_e-\frac{K_1}{2.303}t$	q_t (mg/g)– adsorption capacity at time t K_1 (min^{-1})– the PFO rate constant	Describing the alteration rate of adsorption capacity over time is positively correlated to the gradient between the q_e and q_t (or instant free sites)	[14]
PSO kinetic model	$\frac{t}{q_t}=\frac{1}{K_2q_e^{\ 2}}+\frac{t}{q_e}$	K_2 (g/(mg min)) – the PSO rate constant	Describing the adsorption rate positively relates to the improved useful adsorption sites, while chemisorption is dominant and related to strong interaction (valency forces) of the target contaminant and biochar	[15]
Elovich model	$q_t=\frac{1}{\beta}\ln\left(\alpha\beta\right)+\frac{1}{\beta}\ln(t)$	α (mg/(g min))– the initial sorption constant β (g/mg)– the initial desorption constant	Describing initial heterogeneous surface chemisorption.	[65]
Langmuir isotherm model	$\frac{C_e}{q_e}=\frac{1}{q_m}C_e+\frac{1}{q_mK_L}$	q_m (mg/g)– the maximal adsorption capacity K_L (L/mg)– the Langmuir constant related to the adsorption free energy $R_L=\frac{1}{1+K_LC_0}$	Describing monolayer physisorption occurs at a specific homogeneous surface with fixed active site amounts and the same energy, and free of interactions among the uptake molecules and lateral interactions. R_L values between 0-1 suggest favorable adsorption	[40]
Freundlich isotherm model	$q_e=K_FC_e^{\frac{1}{n}}$	K_F (L/mg)–adsorption bonding energy (or affinity parameter) 1/n– the adsorption intensity coefficient, indicating the adsorption driving force magnitude	Describing non-ideal and reversible multilayer adsorption at heterogeneous surface sites, with exponentially decreased energy distribution, uneven adsorption enthalpy distribution, and improved surface coverage 0<1/n<1 (or high K_F values) suggests favorable adsorption and high adsorption ability 1/n>1 suggests unfavorable adsorption n=1 suggests linear adsorption n=0 suggests unfavorable and irreversible adsorption	[73]

 doi:10.20944/preprints202512.0318.v1

Temkin isotherm model	$q_e = (\frac{RT}{b_T}) ln(K_T C_e)$	b (mol^2/J^2)- the adsorption free energy b_T (kJ/mol)- the Temkin constant K_T (l/g)- the equilibrium binding constant T (K)- the temperature of the adsorption system	Describing the chemisorption on an uneven surface involves adsorbent–adsorbate interaction and the non-uniform and linearly decreased adsorption heat, neglecting the impact of extreme concentration values	[48]
Redlich–Peterson isotherm models	$q_e = \frac{K_R C_e}{1 + a_R C_e^{\theta}}$	K_R (L/g) - Redlich-Peterson constant a_R ($L/mg^{(1-1/A)}$- Redlich Peterson constant θ- the exponent reflecting the heterogeneity of the adsorbent	Describing the combined characteristics of both the Langmuir and the Freundlich models	[37]
Dubinin-Radushkevich isotherm model	$lnq_e = -K_{DR}R^2T^2\left(1+\frac{1}{C_e}\right) + lnq_{DR}$ $E_S = \frac{1}{\sqrt{2K_{DR}}}$	K_{DR} (mol^2/J^2)- a constant indicating the adsorption energy q_{DR} (mg/g)- the adsorption capacity E_S (kJ/mol) – a value crucial to clarify the adsorption mechanisms	Describing whether the adsorption follows the micropore filling mechanism, which is a more general monolayer adsorption model than the Langmuir type. $E_S < 8$ suggests a physisorption $8 < E_S < 16$ suggests an adsorption related to ion exchange $E_S > 16$ suggests a chemisorption	[39]
Weber and Morris model	$q_t = K_P t^{\frac{1}{2}} + C$	K_P (mg/(g $min^{1/2}$))– the intraparticle diffusion constant C – a constant related to the boundary layer thickness	Describing three-step adsorption, *i.e.*, the transfer of adsorbed substrates from liquids to the boundary layer, from the boundary layer to the biochar surface, and intraparticle diffusion into biochar. If the linear plot passes through the origin, intraparticle diffusion is the only controlling step. High intercept favors the adsorption	[55]
Boyd model	$-\ln\left(1-\frac{q_t}{q_e}\right) = K_{bf}\, t$	K_{bf} (1/min)– liquid-film diffusion constant	Describing the transfer of adsorbed substrates from the liquids to the surface of the biochar. If the linear plot passes through the origin, film diffusion is the only rate-limiting step	[34]
Thomas breakthrough curve model	$\frac{C_t}{C_0} = \frac{1}{1+\exp\left(\frac{k_{Th}q_0 m}{v} - k_{Th}C_0 t\right)}$	k_{Th} (mL/(min mg))– the Thomas rate constant q_0 (mg/g)– the adsorption capacity v (mL/min)– the feed flow rate	This model is derived from the Langmuir isotherm and PSO models, describes the adsorption mainly being controlled by interface mass transfer instead of chemical interactions, and is commonly used to predict the column adsorption performance of biochar	[65]
Adams–Bohart breakthrough curve model	$\frac{C_t}{C_0} = \exp\left(k_{AB}C_0 t - k_{AB}N_0\frac{z}{U_0}\right)$	k_{AB} (L/(mg min))– the kinetic constant N_0 (mg/L)– the saturation concentration z (cm) – the bed depth of the fixed bed column U_0 (cm/min)– the superficial velocity	Describing the adsorption rate is limited by external material transfer, the adsorption balance does not achieve instantaneously, and the adsorption capacity of the adsorbent is proportional to the adsorption kinetics, which is generally used to explain the relevance between C_t/C_0 and t in the initiation of breakthrough curves ($C_t/C_0 \leq 0.15$)	[50]
Arrhenius formula	$\ln K_2 = \ln A - \frac{E_a}{RT}$	A- the Arrhenius constant R (8.314 J/(K mol))- the universal gas constant	Describing the effects of temperature on adsorption	[15]
Van't Hoff equation	$lnK_d^{\theta} = \frac{q_e}{C_e}$	lnK_d^{θ} (L/g) is the distribution coefficient	Describing the effects of temperature on adsorption	[5]
Gibbs free energy	$\Delta G^0 = -RTlnK$ $K = \frac{C_e}{q_e}$	ΔG^0 (kJ/mol)- the Gibbs free energy	Negative ΔG° values identify spontaneous adsorption. ΔG° values	[74]

 doi:10.20944/preprints202512.0318.v1

			in the range of 0-20 kJ/mol suggest physisorption	
Enthalpy and entropy	$lnK = \frac{\Delta S^0}{R} - \frac{\Delta H^0}{RT}$	ΔS^0 (kJ/mol)- the adsorption enthalpy ΔH^0 (kJ/mol)- the adsorption entropy	Negative ΔH° values identify exothermic adsorption. ΔH value (67.74 kJ/mol) shows chemisorption. ΔH° of 40-800 kJ/mol and (2.1-40 kJ/mol identify chemisorption and physisorption, respectively. Negative ΔS° values indicate the entropy-decreasing adsorption, high orderliness, low molecule colliding, and low intramolecular and intermolecular degrees of freedom of adsorbed molecules	[12]

3. Preparation and Characterization of Agricultural Residue-Based Biochar

3.1. General Conceptions and Properties of Biochar

Biochar, porous C-rich material, can be prepared via high-temperature (200–1700°C) pyrolysis of biomass (*e.g.*, lignocellulose) under anaerobic, O_2-limited or O_2-free atmospheres, such as inert gas and vacuum environments [12,21,37,39,58]. In general, biochar has a rough surface, irregular shape, condensed structure, relatively high pore volume and surface area (lower than activated carbon), density, greatly aromatized and graphitized architectures, and abundant surface functional groups (*e.g.*, -OH, -COOH, -NH_2, and C=O) [22,30,40,75]. Biochar's C contents can be identified as high (≥60%), middle (30%-60%), and low (10%-25%) [21,46,48]. Biochar has the strengths of rich C content, stable C structure, abundant precursors, sustainable production, renderability, high cost-effectiveness, convenient modification and surface functionality, high catalytic activity and thermal stability, high accessibility for dissolved pollutants, and can remove both inorganic metal ions and organic contaminants [12,38,42,75]. The limitations of biochar include poor affinity, low selectivity, and small co-adsorption capacity [46,75].

3.2. Preparation of Agricultural Residue-Based Biochar

Various approaches have been developed for the biochar preparation, including conventional high-temperature carbonization [32,42,76], microwave-assisted high-temperature carbonization [16,33,77], strong acid carbonization [78], conventional hydrothermal carbonization [15,16], and microwave-assisted hydrothermal carbonization [16] using different agricultural wastes as precursors at present. Different agricultural wastes have different elemental compositions and thus exhibit different properties [39]. In general, these agricultural wastes require pre-treatment to clean and dry the material, and to small and uniform the size, as shown in Figure 2 [4].

Conventional carbonization is often operated at high temperature under inert gas atmosphere or vacuum conditions at open or closed systems using a muffle furnace, tubular furnace, curable tube, heat pipe reactor, top-lit updraft two-barrel furnace, portable charring kiln, microwave oven, and so forth [12,22,42,46,58,79]. According to the preparation conditions, pyrolysis can be divided into slow pyrolysis (300-700°C, several hours, 35-50 wt% of yields), fast pyrolysis (400-600°C, <10 s, <30 wt% of yields), and flash pyrolysis (about 1000°C, <3 s, <20 wt% of yields) [58]. The dynamic molecular structures of the biochar produced at different pyrolysis temperatures are presented in Figure 3.

Unlike pyrolysis under atmospheres, vacuum decomposition induces faster volatile removal, slighter pore blockage, lower loss of surface groups, and shorter combustion duration, followed by greater yields and properties of the biochar [1]. Hydrothermal carbonization is usually performed by mixing the precursor with less solvent (*e.g.*, distilled, acidified, or alkaline water and or organic reagents), subsequently reacting under high temperature (80–250°C) and pressure (2–6 MPa) [15,16]. Microwave heating can assist both the regular and hydrothermal carbonization owing to the distinct heating ways [14–16,47,81]. These approaches have been described in detail in our previous works [14–16,47]. Additionally, the molten salt method has also been used, in which micro-pores are formed

 doi:10.20944/preprints202512.0318.v1

via the partial oxidation of components under high temperature and air atmospheres, while larger pores are formed thanks to the etching and the template impacts of the molten inert salts [49]. Among the above-mentioned approaches, the conventional high-temperature carbonization has been widely applied for biochar preparation [43,82]. The limitations and merits of these approaches for the preparation of biochar are compiled in Table 3. The optimal strategy heavily depends on the properties of biomass (*e.g.*, moisture content, composition, type of agricultural wastes) and the intended application of the biochar (*e.g.*, soil amendment, adsorbent, catalyst).

Figure 2. Pretreatment of agricultural wastes for the preparation of biochar. Reprinted from ref. [72]. Copyright (2025), with permission from Elsevier.

 doi:10.20944/preprints202512.0318.v1

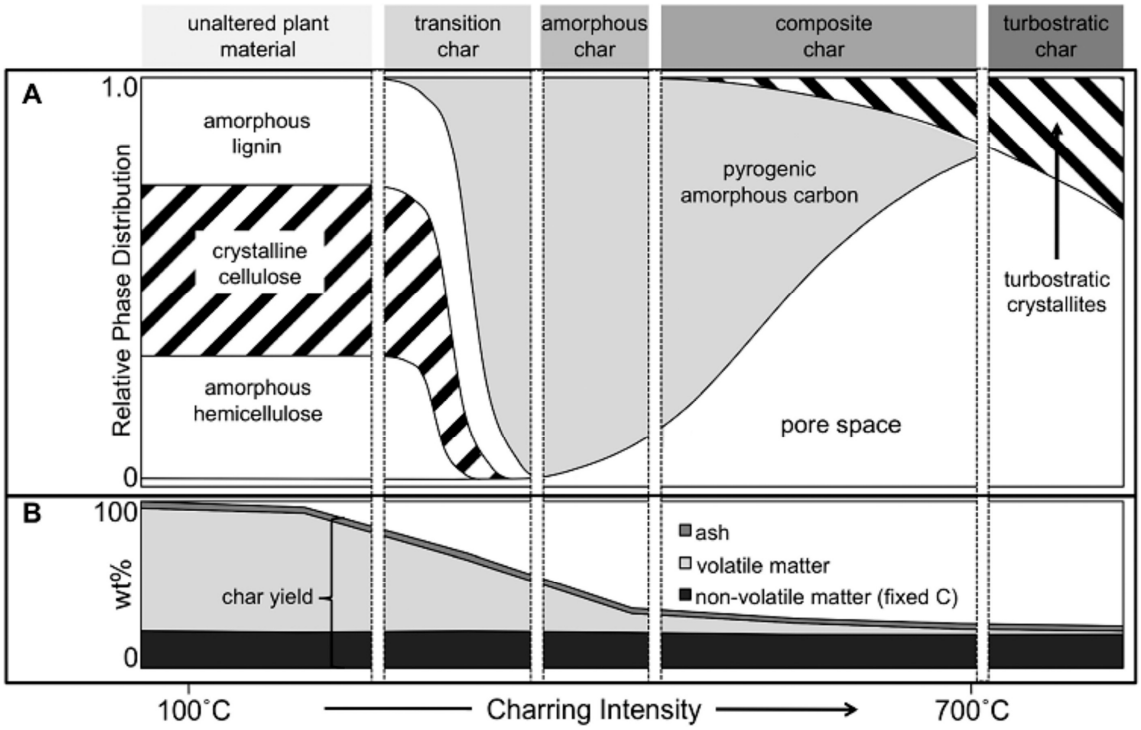

Figure 3. Dynamic molecular structure of the biochar produced at different pyrolysis temperatures. Schematic representation of the four proposed char categories and their individual phases. Reprinted from ref. [80]. Copyright (2015), with permission from ACS.

Table 3. The merits and limitations of developed strategies for biochar preparation [14–16,47,49,81].

Strategies	Merits	Limitations
Conventional high-temperature heating (pyrolysis)	Most common and well-established method. Can use a variety of feedstocks. Higher temperatures (above 500°C) yield highly stable carbon and porous biochar with high fixed carbon content. Products (bio-oil, syngas, and biochar) can be used for energy.	Longer processing times (especially slow pyrolysis). Heat transfer can be slow and non-uniform, particularly in large reactors. Requires a significant amount of energy, especially to drive off moisture from wet biomass.
High-temperature heating under vacuum	Lower decomposition temperature and shorter processing time compared to atmospheric pyrolysis. This strategy can potentially increase bio-oil yield and improve product quality by quickly removing volatiles.	Increased complexity and cost due to the need for vacuum equipment. This strategy may require specialized reactor design.
Microwave Calcination (Pyrolysis)	Rapid and uniform heating due to direct energy transfer to the biomass. Shorter processing time and higher energy efficiency compared to conventional heating. Can produce biochar with enhanced microporous structure and surface functional groups.	Potential for hotspots and temperature non-uniformity in large-scale applications. Reactor design and precise control are more complex.
Hydrothermal synthesis (hydrothermal carbonization)	Uses wet biomass directly (no pre-drying needed), which is an advantage for high-moisture feedstocks. Operates at lower temperatures (180 to 250°C)	Requires specialized equipment (autoclaves) to handle high pressure. Longer reaction times (hours to days). Hydrochar may

 doi:10.20944/preprints202512.0318.v1

	under high pressure. Produced hydrochar is carbon-rich but often less stable than pyrolysis biochar.	have lower C-stability and surface area than high-temperature biochar.
Microwave hydrothermal synthesis	Combines the benefits of microwave heating with hydrothermal carbonization. Offers significantly reduced reaction time (hours to minutes) and homogeneous heating compared to conventional hydrothermal carbonization. Allows for rapid and precise process control.	Requires specialized microwave equipment designed for high-pressure hydrothermal conditions. Cost and scalability can be challenging.
Salt-melting method (molten salt pyrolysis)	Molten salts can act as pore-forming agents or activating agents to produce biochar with high specific surface areas and enhanced properties (e.g., magnetic biochar). The salt can often be recovered and reused, promoting sustainability.	Introduces a new chemical, i.e., salt, into the process, requiring a separation step to recover the salt and clean the biochar. Higher complexity and potential for secondary pollution if not properly managed.

During the preparation processes, the biomass undergoes melting, softening, vesicle formation, and decomposition with gas emission [49]; the light organics of biomass precursors are highly reacted and disrupted via volatilization [21]; the hemicellulose and cellulose usually decompose at 200-300°C and 300-400°C, respectively (the mechanism of lignin, hemicellulose and cellulose pyrolysis during biochar preparation are shown in Figure 4) [49]; the existing metal components may accelerate the pyrolysis of the biomass and improve the porosity of biochar [26,83]; the oxidation induces low ash components and high gas emission under air atmosphere [54]; the pH_{PZC} value can be increased (due to the elimination of acidic O-containing groups, like -COOH, -OH, and R−CH=O), and yields of C and biochar can be improved (due to low oxidation) under high temperatures and limited O_2 atmosphere [26,84]; the exterior of biomass usually suffers more rapid decomposition compared to the inside part, leading to visible cracks and the exposure of the inner Si-containing structure [85]; the aromatic groups can be formed via the condensation and pyrolysis of lignocellulosic [35]; and the C yield and ash fractions relate to the lignocellulose contents in the precursors [21]. Moreover, the porous structure of biochar can be blocked by tarry and alkaline metal components during the biomass preparation [40].

Precursor type, carbonization strategies, heating approaches (temperature, way, rate, and holding duration of heating), and carbonization atmosphere (*e.g.*, air, N_2, Ar, vacuum, and adiabatic conditions) can influence the physicochemical and structural properties of biochar [22,54,58,79]. Various precursors include different metals, inorganic, and organic components, impacting the pH_{pzc} value, morphology, and C/H and C/O ratios of biochar [84]. Wood-based biochar is usually reported to exhibit higher stability and better surface and adsorption properties than the others [55]. Alkali metals in the precursor help broaden the biochar lattice and the pore size [41]. Mg and Ca remaining in biochar after pyrolysis favor cation adsorption via ion exchange [52,53]. SiO_2 and its content in precursors, especially for rice husk, have been reported to promote the texture, architecture, and porosity of biochar [26,85]. SiO_2 can also react with H_2O to produce Si-OH on the biochar's surface, which favors adjusting its surface charge at different pH values [48]. Biochar's hydrophobicity, aromaticity, and graphitization improve with the augmented carbonization temperature [40]. On the other hand, these metal components may induce the reduction of biochar's surface area and the obstruction of its pores [35]. Low carbonization temperatures (< 400°C) lead to low specific surface area (<10 m^2/g), but favor protecting the functional groups, increasing the hydrophilicity of biochar (due to the preservation of O-containing groups) and the removal of polar or inorganic contaminants via surface functional group-induced precipitation, ion exchange, and electromagnetic gravity [20,58,84]. In contrast, raising the temperature (500-700°C) highly improved the surface area (>100

 doi:10.20944/preprints202512.0318.v1

m^2/g), pore volume, and porosity owing to the rapid generation of volatile substances (*e.g.*, H_2, CO, and CH_4), the sufficient discharge of them, decomposition of by-products in pores (*e.g.*, tar oil), and the occurrence of aromatic condensation [26,41,74]. Nevertheless, high carbonization temperatures are not always beneficial. Excessive temperature (>700°C) could decrease the surface functional group (*e.g.*, C=O, -COOH, -OH) content via dehydration and deoxygenation, reduce the surface area and yield of biochar, increase the alkalinity of biochar (due to the removal of acidic groups), rise the pH_{pzc} of biochar (since the dehydration and decarboxylation and the presence of basic carboxylate and hydroxide groups) intensifies), disrupt the biochar's structure, and limit the subsequent adsorption ability [26,46,49,55,74]. The C content of biochar can be improved via H_2SO_4 and sonication treatment in sequence [78].

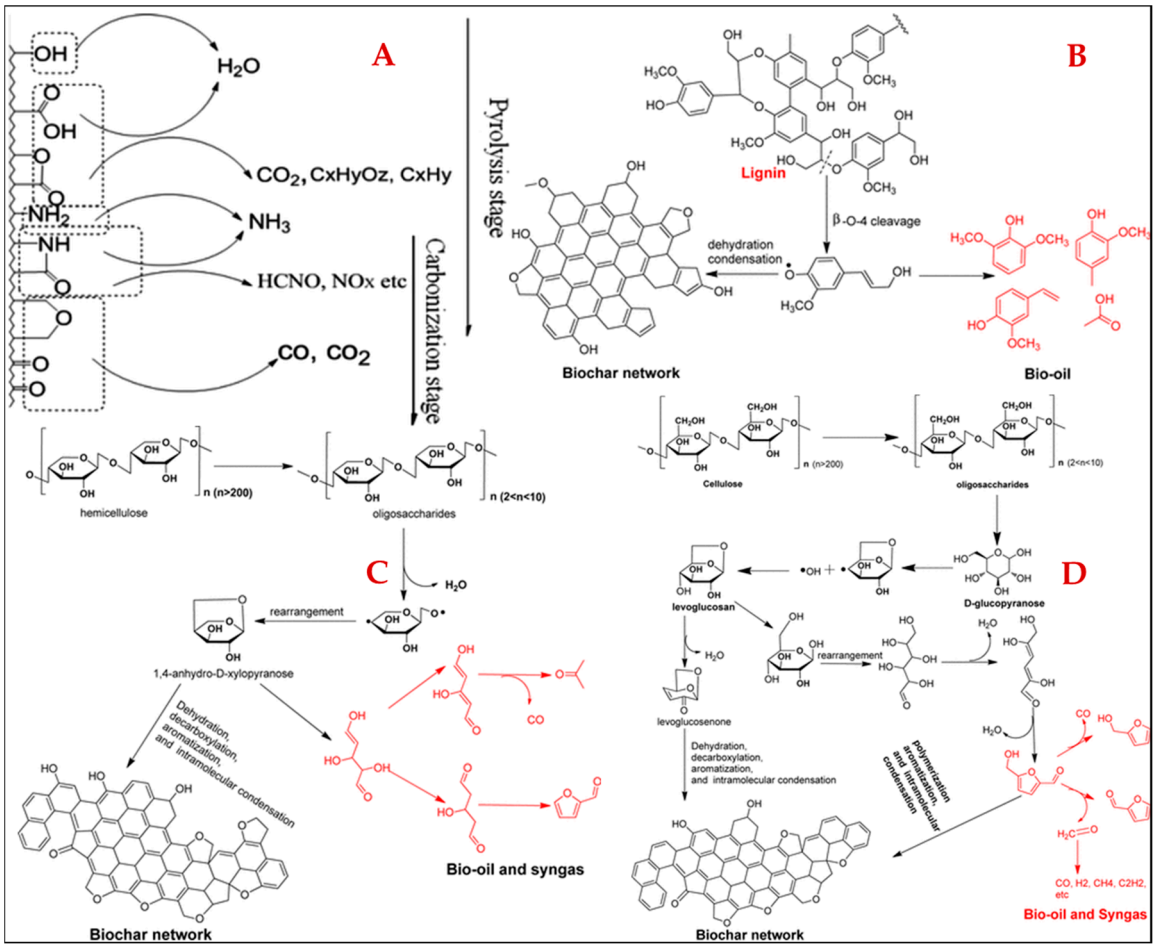

Figure 4. Decomposition of biomass with the increase in pyrolysis temperature (A); the pyrolysis mechanisms of lignin (B), hemicellulose (C), and cellulose (D). Reprinted from ref. [80]. Copyright (2015), with permission from ACS.

3.3. Improved Fabrication of Agricultural Residue-Based Biochar

The physicochemical processing, including activation, modification, and functional of biochar, favors the improvement of its surface and pore properties [40,46]. In general, biochar can be chemically and physically activated using KOH, K_2O, NaOH, $NH_3 \cdot H_2O$, $MgCl_2$, $ZnCl_2$, $CaCl_2$, HNO_3, H_2SO_4, H_3PO_4, HCl, CO_2, steam, *etc.* [15,16,22,39–42]. Compared to chemical activation (450-900°C), physical activation commonly requires a higher temperature and longer duration [41]. Chemical treatment can increase the pH_{pzc} through protonating the functional group and removing carbonates and hydroxide in biochar [46]. Particularly, activation using $NH_3 \cdot H_2O$ can trigger the dehydration, decarbonization, and dehydrogenation of substances containing C=O, changing the H/C and C/O fractions and introducing basic N-containing groups [75]. Activation using CO_2 can induce the

 doi:10.20944/preprints202512.0318.v1

oxidation of biochar and introduce O-containing groups [83]. Nevertheless, the use of these activators could cause negative environmental effects and low cost-effectiveness. For instance, $ZnCl_2$ is known as a toxic activator, which may induce secondary pollution and pose potential environmental risks. Biochar has been functionalized using a variety of modifiers, like CS_2, sodium alginate, cellulose, chitosan, coal fly ash, inorganic elements (*e.g.*, N and S), and transition metal (*e.g.*, La) and their salts (*e.g.*, Fe_3O_4) [5,25,31,38,50,83,86]. Specifically, incorporating sodium alginate in biochar can enhance metal cations adsorption via coordination interactions [87]. Coal fly ash is conductive to promoting the surface aromaticity and hydrophobicity, and reducing C=O but protecting R1(R2)C=O groups [83]. S-doping is conducive to immobilizing the metals and introducing functional groups (*e.g.*, S^{2-} and SO_3^{2-}) [50]. N-doping can enhance the surface polarization and electrostatic attraction of metal cations [49,50]. Metal-doping into biochar can decrease the electronegativity and alter the surface charge distribution, and thus improve its affinity [30]. La-doping in biochar can enhance the specific affinity of PO_4^{3-} [63]. Fe-doping could promote various properties of biochar, such as surface texture, magnetism, surface charge density, mechanical strength, thermal stability, redox ability, *etc.* [38,58]. Ca-doping contributes to broadening the pH suitability of biochar, as well as improving the biochar decomposition, improving the porosity, and supporting the Fe-doping [58,88]. However, the modifiers may lead to some adverse effects on biochar, *e.g.*, the blockage of pores, the decrease of the surface area, and the reduction of the economic efficiency, yield, and effectiveness of biochar (Figure 5) [50]. In addition, recyclability and regeneration of biochar are crucial for evaluating its stability, economic efficiency, sustainability, feasibility, and practicality [1]. Most of the developed biochar or their composites exhibit excellent reusability, with low reduction of the adsorption capacity after at least three adsorption-desorption cycles [5]. The decrease in adsorption capacities of biochar after several adsorption-desorption cycles has been frequently reported, which can be attributed to the inactivation of certain adsorption sites owing to the reduced surface area and pore obstruction after thermal processing, the disruption of surface functional groups and the loss of some functional elements (*e.g.*, N, S, and mental) by solvents and under high temperature processing, incomplete desorption due to the strong bonding, and the interference of other compounds in wastewater [31,36,46,50,89]. The consumed biochar can be regenerated via high-temperature treatment (*e.g.*, 150°C [46]) and solvent elution (*e.g.*, 30% EtOH, distilled water, 0.1 M EDTA, HCl, NaOH, HNO_3, and H_2SO_4 solutions), which favors the valorization of waste biochar and the removal of the secondary pollution risk from the enriched contaminants in biochar [12,15,21,22,31,46,74,78].

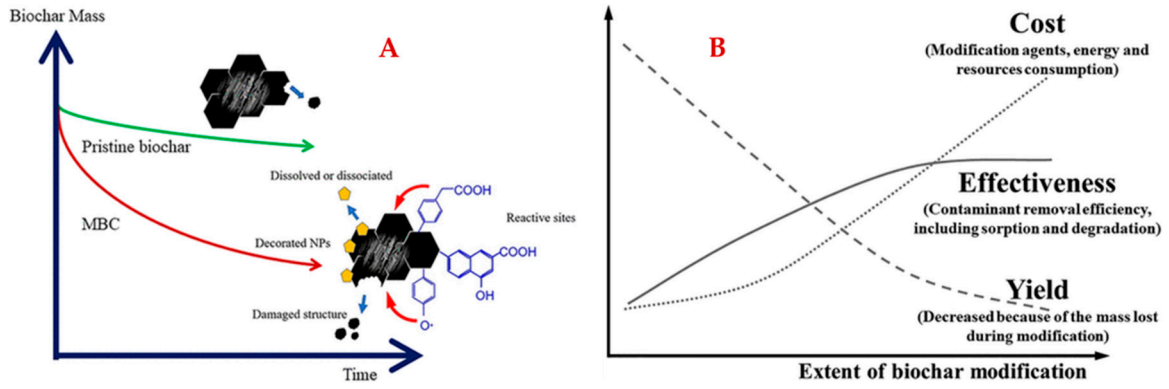

Figure 5. Effect of modification on the carbon structure stability (A) and the cost, effectiveness, and yield (B) of biochar. Reprinted from ref. [90]. Copyright (2021), with permission from ACS.

3.4. Characterization of Biochar

Usually, the physicochemical properties of biochar can be clarified using Fourier-transform infrared spectroscopy (FT-IR), Brunauer–Emmett–Teller (BET) surface analysis, scanning electron microscopy (SEM) characterization, energy-dispersive X-ray spectroscopy (EDS, also known as elemental analysis), zeta potential measurement, X-ray diffraction (XRD), X-ray photoelectron

 doi:10.20944/preprints202512.0318.v1

spectroscopy analysis, and Thermogravimetric Analysis (TGA) [14,16,47]. FT-IR analysis of biochar before and after adsorption favors clarify the chemical interaction and functional groups that contribute to the effective adsorption, as well as the adsorption mechanism. BET analysis offers the porosity information of biochar, including specific surface area, pore diameter distribution, micropore, mesopore, and total pore volumes. The pore size in biochar can be divided into micro- (<2 nm), meso- (2-50 nm), and macro-pores (>50 nm) based on the International Union of Pure and Applied Chemistry (IUPAC) [14,15,84,91,92]. Mesopores of biochar are of great importance for sufficient active sites, ensuring better diffusion and mass transfer [74]. SEM images present the morphology and texture of the biochar surface, such as porosity, granularity, roughness, construction (*e.g.*, multi-layer, spherical, tube, and core-shell structure), *etc.* EDS analysis can deconstruction the element composites of the biochar surface, especially useful when combined with the SEM analysis. Zeta potential analysis facilitates the illustration of the pH effects and the adsorption mechanism (*e.g.*, electrostatic interaction between the surface of biochar and substrate molecules) [6]. The pH_{PZC} value relates to the pH of liquids (pH_L) where biochar's surface is free of charge. Biochar's surface is negatively charged as $pH_L > pH_{PZC}$, and vice versa [84]. Combining various characterizations with the adsorption properties helps to interpret the adsorption mechanisms comprehensively. XRD can identify the crystal phase composition of biochar. Crystallinity can affect biochar's reactivity, porosity, and stability, thereby impacting its performance in various environmental and agricultural applications [30,55]. XPS analysis can determine the atomic composition, contents, valence, bonding patterns, and surface properties in the biochar [1,6,26]. TGA analysis was conducted to evaluate the thermal stability and degradation behavior of the biochar over a range of temperatures. It provided insights into temperature-dependent changes in weight and helped understand the decomposition patterns of the biochar under different conditions [55].

4. Use of Agricultural Residue-Based Biochar for Wastewater Remediation

Agricultural waste-biochar adsorption is a low-cost and effective wastewater remediation strategy, able to remove different contaminants, including dye, antibiotics, pesticides, pharmaceutical residues, heavy metal ions, nutrient substances, and organic carbon, as well as improve the wastewater quality (*e.g.*, turbidity, chroma, smell, pH value, and toxicity) [35]. The adsorption capacity of biochar is commonly lower in wastewater than in clean water due to the competitive adsorption among the target compounds with other contaminants, caused by the complex composites of wastewater [57]. Thus, biochar has been combined with other materials, *e.g.*, poly(*N*-hydroxyethylacrylamide) hydrogel, to achieve better decontamination performance of wastewater [3,51,93,94]. Adsorption decontamination favors decreasing the total solids (TS), total suspended solids (TSS), total volatile suspended solids (TVSS), Total Dissolved Solids (TDS), total organic carbon (TOC), biochemical oxygen demand (BOD), and chemical oxygen demand (COD) of wastewater [16,37,39]. Meanwhile, the recovered macronutrients such as N, P, and K (in the forms of ammonium, nitrate, phosphate, and potassium salts) from certain types of eutrophication wastewaters like human urine, septic tank wastewater, blackwater, and biogas wastewater via adsorption can be reused to support the growth of crops [26,27,46]. Similarly, the recovery of phenolic compounds from olive mill wastewater and N and S from latex industrial wastewater can also be further valued [37,79]. Generally, the adsorption decontamination performance of wastewater by agricultural waste-based biochar depends on the preparation processes (*e.g.*, the pyrolysis temperature, gas atmosphere, and heat approaches), the target substrates, the complexity of liquids, the operation properties like dosage of adsorbents, volume of liquids, reaction temperature, content of contaminants, pH of the matrix, contact duration, adsorption mode (batch and column modes), *etc.* [16,72].

In wastewater, various conditions, such as initial contaminant concentration, connection time, dosage of biochar, pH, and temperature of the adsorption system, and co-existing ions, can influence the adsorption performance of the biochar. Generally, high initial concentrations favor adsorption due to the large concentration gradient and high driving force leading to great interphase mass

 doi:10.20944/preprints202512.0318.v1

transfer, intrapore molecule diffusion, and improved affinity of biochar towards the target compounds, followed by rapid adsorption with high capacity [1,11,63,74,95]. At the initiation of adsorption, the process proceeds rapidly, attributed to the sufficient and accessible adsorption sites, a high concentration difference driving force, and low diffusion resistance. With prolonged connection time, the adsorption will gradually slow down due to the limited adsorption sites and low mass transfer and molecular diffusion. Eventually, a dynamic adsorption-desorption equilibrium will be reached, where the total adsorption capacity becomes stable, and the adsorption site may continue the empty-occupy cycle, and the adsorbed compounds might influence the remained ones in liquids via electrostatic repulsion, size exclusion, or other weak interactions [1,2,21,37,50,74]. High dosages of biochar do not always favor adsorption. Appropriate dosages can not only offer enough surface adsorption sites and ensure economical and fast operation but also avoid the biochar congestion [11,30,31,50]. The influence of pH on adsorption is complex. For biochar, the pH of adsorption systems can change the types and distribution of biochar's surface charge via altering the zeta potential of biochar relative to its pH_{pzc} and the dissociation of chemical groups of biochar's surfaces, and thus affecting the electrical interactions with the target substrates in liquids [1,5,54]. It has been reported that the alternation of biochar's surface charge can promote its adsorption selectivity [46]. For the target substances (*e.g.*, dyes, TC, phosphorates, ammonium, and Fe ions), especially the amphoteric compounds, pH can change their existence form (molecule or ion) in liquids, and thus impact their affinity with biochar [6,11,30,84]. Usually, acidic conditions (pH 5-6) favor metal sorption, whereas alkaline conditions facilitate the organics and PO_4^{3-} sorption [58,85]. Under very acidic conditions, competitive adsorption between target compounds (*e.g.*, metal ions and NH_4^+) and H^+ and electrostatic repulsion will occur, limiting the adsorption [11,49,50]. Under alkaline conditions, organics are highly ionized, allowing high mitigation and diffusion of them [85]. Alkaline conditions favor biochar adsorption by promoting their surface negative charge density and enhancing the induced electrostatic interaction [58,84]. Alkaline conditions also favor cation adsorption via electrostatic attraction, surface complexation, and precipitation, but inhibit anion adsorption via the competitive adsorption of OH^- ion and electrostatic repulsion [21]. High temperature is conducive to endothermic adsorption, while low temperature is conducive to exothermic adsorption. However, high temperatures can decrease the adsorption interaction and intensify molecular motion, which may result in the desorption of substances [1,11]. The effect of temperature can be detailed via the thermodynamic investigations [14,15,47]. The co-existing ions (*e.g.*, Cl^-) change the ionic strength of the liquids, impacting the adsorption via the salting-out effect, molecular dissociation, competitive adsorption, and electrostatic screening effect [46,50]. Thus, the optimal adsorption conditions are crucial for the desired adsorption performance.

The optimized adsorption of various contaminants from wastewater using biochar derived from various agricultural wastes is summarized in Table 4.

Table 4. The adsorption of contaminants from wastewater using biochar derived from agricultural residues.

Precursors of biochar	Pollutants	Wastewater	Fabrication conditions of biochar	Adsorption conditions	Surface area, pore size, total pore volume	Functional groups and mechanisms	Adsorption capacities	RE (%)	Refs.
Date seed	Carbendazim	Municipal wastewater	550°C, 0.5 h, N_2 atmosphere	3 g biochar/L, pH 7, 40 min, 200 mL, 1 mg/L	307.5 m^2/g, 3.80 nm, 0.278 cm^3/g	-OH, -COOH, -Ph π–π electron donor–acceptor interactions, π–π stacking, dipole–dipole interactions, pore filling, electrostatic attraction, H-bonding	-	88.7	[4]
	Linuron							85.9	
Corncob	N, P, K	Human urine	600°C, anaerobic condition	60 g biochar, 600 mL, 5 days	1.7 m^2/g, -, 0.0005 cm^3/g	-OH, -COOH, C=C ion exchange, chemical interaction	1200, 242.8, 43.7 mg/L	-	[27]
		Biogas wastewater					342.4, 105, 35 mg/L		
Groundnut shells, drumstick	BOD	Pharmaceutical	Groundnut shell: 500°C, 4 h;	35 g biochar mixture (1:1:1),	-	OH, $-CH_3$, C-H, C=C, C-OH, C=O -	-	72.1	[72]

 doi:10.20944/preprints202512.0318.v1

seeds, coconut fiber		wastewater	drumstick seeds: 600°C, 2 h; coconut fiber: 700°C, for 2 h	443.6 mg/L, pH 7, 25°C, 1.5 h					
Coconut shells	Methylene blue	Dye wastewater	-	20 mg Fe_3O_4/biochar /sodium alginate aerogel beads, 50 mL, 50 mg/L, 150 rpm, 25°C, 24 h, pH 7	152.5 m^2/g, 2.60 nm, -	-OH, -COOH pro-filling, H-bonding, electrostatic interaction	-	-	[5]
Rice husk	TC	Human urine	-	0.1 g biochar/mL, 5 days	4.63 m^2/g, -, -	–OH, C-H, C-O, C=C H-bonding, ligand exchange, ion exchange, electrostatic interactions	-	60-80	[26]
	N, P, K						236.5, 256.7, 4.6 mg/L	50, 70, 80	
Peanut shell	Atrazine	Synthetic wastewater	450°C, 4 h	20 mg biochar, 25 mL, 20 mg/L, 150 rpm	61.8 m^2/g, 1.96 nm, 0.03 cm^3/g	-OH, NH_2, C-O, C=O, C-H, C=C, C-C π-π interactions, H-bonding	2.8 mg/g	-	[6]
Coconut shell	Ammonium, nitrate, phosphate	Synthetic wastewater	-	0.5 g biochar, 100 mL, 80 mg/L, 6 h, 80 rpm	-	C=C, C-O-C, C=O ion exchange, chemical interaction	10.12, 7.51, 10.79 mg/g	-	[20]
Eucalyptus bar	Anthraquinon	Dye wastewater	500°C, 1.5 h, anaerobic condition	0.913 g biochar composite/L, 21 mg/L, pH 3.9, 117 min	57.4m^2/g, 1.48 nm, 0.41 cm^3/g	Si-OH, Si-N, -COOH, -OH, C-O-C, C=O π–π interaction, electrostatic attraction, surface functional groups, chemisorption, pore-filling	-	-	[48]
Walnut shell	Quinoline	Coking wastewater	500°C, 2 h, N_2 atmosphere	10 mg KOH-activated biochar, 50 mg/L, 25°C, 50 mL	969.8 m^2/g, 2.34 nm, 0.4 cm^3/g	C–O–C, C-O, C=OC-H, C-C, C=C–OH porous adsorption, π–π interaction, H-bonding, electrostatic attraction	78.2 mg/g	-	[57]
Giant reed	Basic blue 41	Textile wastewater	10 °C /min at 600°C for 2 h, 5 L/min of N_2 flow	4 g biochar/L, 5.7 mg/L, 1 h	429.0 m^2/g, -, 0.09 cm^3/g	C-H, C-O, C-C, C-OH, C=O, C=C electrostatic interactions	5.14 mg/L	90.3	[39]
	Color			4 g biochar/L, 106 Pt–Co, 1 h			83 Pt-Co	89.3	
	Turbidity			4 g biochar/L, 48.55 NTU, 1 h			33.7 NTU	69.4	
	COD			4 g biochar/L, 928 mg/L, 1 h			582 mg/L	62.7	
Mandarin tree pruning	Dissolved organics	Olive mill wastewater	600°C, N_2 atmosphere	5 g biochar, 6800 mg/L, 100 mL, 25°C, 160 rpm	-	- Precipitation, surface complexation, electrostatic interactions, π–π interactions	-	28	[37]
				1 g biochar, 17 g/L, 100 mL, 25°C, 160 rpm			140 mg/ g	-	
Eucalyptus wood	Anthracene	Vehicle-wash wastewater	450°C, 1 h, N_2 atmosphere	0.4 g biochar, 40 ppm, 1 h, pH 5, 50°C	18.4 m^2/g, 1.5 nm, 0.01 cm^3/g	C-H, C=C, C=O Van der Waals dispersive contacts, electrostatic interactions, H- H-bonding	-	98.4	[11]
Rice husks	Mn, Se, Fe ions	Urban wastewater	Biochar in 1 M NaOH ($m_{Biochar}/m_{NaOH}$, 2:1), 12 h, 25°C	0.25 g NaOH-biochar/, biochar/HCl-biochar, 0.303 mg/L Mn, 0.116 mg/L Se, 0.390 mg/L Fe, 50 mL, 200 rpm, 10 h	-	C≡C, C≡N, C=C, C-O, C-H, Si-O-Si electrostatic attraction, ion exchange, complexation, precipitation	-	76, 66, 66	[40]
			Biochar in 10% wt. HCl, 3 h, 500°C at 10 °C/min, 200, 8 h, mL/min of N_2 flow				-	30, 26, 59	
			350°C at 10 °C/min, 6 h, 200 mL/min of N_2 flow				-	3, 39, 48	
Garlic peel	Methylene blue	Industrial wastewater	150°C at 5 °C/min, 2 h, vacuum atmosphere	5 mg biochar, 20 mL, 50 mg/L, 1 h, 25°C	5.46 m^2/g, 1.49 nm, 0.18 cm^3/g	O-H, C=O, C-O, C=C-H Electrostatic attraction, H-bonding, π-π stacking	14.33 mg/g	-	[1]
Corn stover	Phosphate	Pig farm wastewater	500°C, 2 h, N_2 atmosphere	0.2 g Ce-modified biochar, 100 mL, 24 h, 180 rpm, 25°C	14.1 m^2/g, 7.05 nm, -	-CH_2-, -CH-, Ce-O surface precipitation, ligand exchange,	27.96 mg/g	43.3	[30]

 doi:10.20944/preprints202512.0318.v1

						complexation, electrostatic attraction			
Lotus leaf	Be ion	Simulated beryllium mining wastewater	600°C, 3 h	0.05 g PO_4^{3-}/NH_4^+ modified biochar, 50 mL, 35°C, pH 5.5, 16 h, 175 rpm	4.927 m^2/g, 3.86 nm	Phosphoric acid, ammonia, -OH surface complexation and precipitation, pore filling,	40.38 g/kg	-	[75]
Palm leaves	Tetracycline	Synthetic wastewater	500°C, 2 h, 10 °C/min under N_2 atmosphere	1 g biochar/L, 20 mL, 0.5 mg/L, 180 rpm, pH 5.7, 24 h, 25°C	31.5 m^2/g, 5.38 nm, 0.03 cm^3/g	-COOH, -OH, C=O, C-O, C=C, C-H H-bonding, π-π interaction, electrostatic interaction, pore-filling	-	80	[2]
Prosopis juliflora	Sulfamethoxazole	Industry wastewater	600°C at 10 °C/min, 2 h, N_2 atmosphere	1 g biochar/L, pH 5, 5.3 mg/L, 2 h	875 m^2/g, -, -	-OH, -COOH, -Ph, C-N, C-H, C-Cl, C-O electrostatic interactions, H-bonding, π-π stacking	-	76.7	[55]
	Ciprofloxacin			1 g biochar/L, pH 5, 8.3 mg/L, 2 h				80.4	
	COD			1 g biochar/L, pH 5, 2.5 g/L, 2 h				79.4	
	TOC			1 g biochar/L, pH 5, 1.05 g/L, 2 h				88.2	
Oil palm fronds	COD	Latex industrial wastewater	300-438°C at 13 °C/min, 3 h	15 g Biochar/L, 4 h, 150 mL	68.98 m^2/g, 1.68 nm, -	O-H, C=C, C-H, C-O, S=O, Si-O-Si, S-S Ion exchange, H-bonding	-	41.2	[79]
	Suspended solids							87.6	
	Sulfate							58.8	
	Sulfide							56.8	
Bamboo	Phosphate	Phosphate fertilizer plant wastewater	900°C at 8 °C/min, 2 h, N_2 atmosphere	Iron/CaO-modified biochar, 1660 mg/L, 48 h	146.5 m^2/g, 2.78 nm, 0.1 cm^3/g	- Chemical precipitation	-	~100	[58]
Fronds and leaves of date palm	Phenol	Synthetic primary-treated wastewater	600°C at 8 °C/min, anaerobic condition	0.1 g biochar, pH 6, 20 h, 800 mg/L, 50 mL, 200 rpm	245.8 m^2/g, 4.6 nm, 0.12 cm^3/g	O-H, C=C, C-H, Si-O, -COOH π-π interactions, H-bonding, pore filling, electrostatic interaction	241 mg/g	60.3	[74]
		Synthetic secondary-treated wastewater		0.1 g biochar, pH 6, 20 h, 52 mg/L, 50 mL, 200 rpm			22.28 mg/g	85.7	
Parthenium hysterophorus	Cr ion	Tannery wastewater	500°C, 2 h	Fe_3O_4/biochar,85.13 mg/L	237.4 m^2/g, -, -	O-H, C-O-C, C-OH, Fe-O, Van der Waals forces, H- H-bonding, hydrophobic interactions	-	81.8	[38]
Corn straw	Cr ion	Industrial wastewater	500°C, 2 h, Ar atmosphere	0.05 g Fe_3O_4/biochar, 32.8 mg/L, 3 h, pH 6	508.4 m^2/g, 4.6 nm, 0.55 cm^3/g	Fe–O, Fe–OOH, C=O, O–H Surface physisorption, pore filling, and electrostatic interaction	-	72.6	[31]
Citrus trees	Tetracycline	Industrial wastewater	-	3.5 g biochar, 50 mL, pH 4, 90 mg/L, 20°C	364.9 m^2/g, 1.08 nm, 0.2 cm^3/g	O-H, C=C, C=O, C-H, C-Cl π-π interaction	-	95	[12]
Corncob	Ammonia	Livestock wastewater	450°C for 1.5 h, 4 °C/min	0.3 g, 50 mL, 6.2 mg/L pH 12, 1.5 h	-	-	-	83.98	[96]
Corn Stalks	COD	Hospital wastewater	400-500°C	56.0 mg/L	-	-	-	57.1	[29]
	BOD			46.8 mg/L				56.8	
Wheat straw	Inorganic-N	Simulated agricultural wastewater	450°C at 5 °C/min, 5 h, 400 mL/min of N_2 flow	10 g Mg-modified biochar/L, 24 h, 250 mL, 25°C, 80 rpm	23.4 m^2/g, -, 0.062 cm^3/g	C=C, -OH, -Ph -NH_2, -COOH H-bonding, π-π/n-π interaction	4.44 mg/g	-	[46]
Palm bunch	Methyl paraben	Secondary wastewater effluent	450°C at 10 °C/min, 0.5 h, 400 mL/min of N_2 flow	H_2SO_4-activated biochar	60.3 m^2/g, -, 0.54 cm^3/g	C=C, -OH, C=O, S=O, C≡C Channel diffusion, H bonding, Van der Waals force, n-π/π-π interaction	-	80.3	[97]
	Carbamazepine							79.9	
	Ibuprofen							70.2	
	Triclosan							74.3	
Rotten sugarcane bagasse	Pb ion	Stimulated wastewater	600°C, 2 h, air atmosphere	30 mg biochar, 50 mg/L, pH 5	391.9 m^2/g, 20.9 nm, 0.532 cm^3/g	-COOH, CHO, C=O, C-H, C=C, O-C=O Ion exchange, surface complexation/function group coordination, precipitation, π-π interaction	-	97.3	[49]
	Cu ion							99.8	
	Cr ion							100	
Wheat straw	COD	Dye industry wastewater	300-500°C	2.5 g biochar/L, 25 mL, pH 7.62, 150 rpm	-	C=C, C=O, C-H, C-O-C, -OH, -COOH Ion exchange, Surface physisorption, electrostatic interaction, complexation	-	62	[22]
Rice husk	Pb ion	Industrial wastewater	500°C at 5 °C/min, 2 h, N_2	Biochar, 35.7 mg/L, pH 6.68, 100 mL	63 m^2/g, -, 0.381 cm^3/g	C-H, C=O, -OH, C-O Ion exchange, surface physisorption,	-	63.8	[25]

 doi:10.20944/preprints202512.0318.v1

			atmosphere			electrostatic interaction, complexation			
Auricularia auricula spent substrate	Cd ion Cu ion Zn ion	Electroplating wastewater	500°C, 2 h, anoxic conditions	0.1 g CS_2-modified biochar/L, 5.21 mg/L Cd^{2+}, 1.11 mg/L Cu^{2+}, 48.72 mg/L Zn^{2+}, 25°C, pH 5.59, 2 h	2.54 m^2/g, 13.4 nm, 0.009 cm^3/g	C-S, -OH, S=C=S, C=O, -NH_2 Complexation, precipitation	14.01 mg/g 13.56 mg/g 50.19 mg/g	-	[50]
Coffee husk	Ammonium	Domestic wastewater	350°C, 1 h	20 g biochar/L, 130 rpm, 6 h, 108 mg/L, pH 7.4	0.43 m^2/g, -, -	-OH, C-H, C=O, C=C, -COOH Complexation, ion exchange, H-bonding, electrostatic attraction	-	20	[84]
Maize stalk, black gram, pine needle, Lantana camara	COD TSS Ammonia Total K&N Total K As ion Cd ion Cr ion Pb ion Zn ion Cu ion	Municipal wastewater	600°C at 10 °C/min, 4 h	5 g steam-activated biochar, 5 days	38.9-43.9 m^2/g, 2.74-3.96 nm, 2.47-3.99 cm^3/g	-COOH, -OH, -NH_2 Electrostatic interaction, precipitation, surface complexation	-	88-91 81-85 87-91 59-69 78-88 79-87 53-95 83-88 78-95 90-95 93-96	[35]
Rice straw	COD BOD COD BOD	Livestock wastewater	300°C, 6 h	Batch mode, 4 g biochar/L, pH 9 Batch mode, 4 g biochar/L, pH 9 Column mode, 373 mg/L COD, 105 min Column mode, 240 mg/L BOD, 105 min	35.4 m^2/g, -, 0.36 cm^3/g	- Polarity, hydrophobic/aromatic interaction, and molecular size	-	40 40 79 84	[85]
Jujube seeds	TSS TDS Ni ion Zn ion Cu ion Cr ion	Electroplating industrial wastewater	Jujube seeds/H_2SO_4, 1:3 for 4 h, sonication 20 min at 24 kHz	2 g biochar/L, pH 1 h, 30°C, 20 mg/L 2 g biochar/L, pH 1 h, 30°C, 2.8 g/L 2 g biochar/L, pH 1 h, 30°C, 15 mg/L 2 g biochar/L, pH 1 h, 30°C, 20 mg/L 2 g biochar/L, pH 1 h, 30°C, 40 mg/L 2 g biochar/L, pH 1 h, 30°C, 70 mg/L	48.32 m^2/g, -, 0.16 cm^3/g	-OH, C=C, C=O, C-OH, La-OP-, -CO= Ligand exchange, electrostatic attraction, complexation	-	10 0.79 99.9 ~100 ~100 ~100	[78]
Coconut husk Rice husk Coffee husk	NO_3-N and NO_2-N	Slaughterhouse wastewater	700°C, 6 h, under N_2 atmosphere	1.5 g biochar, 26°C, pH 7.35, 50 mL, 120 rpm, 2 h	6.84 nm 1.97 nm 1.63 nm	-OH, C=C, Si-O-Si ligand exchange, electrostatic attraction, complexation	0.2-13 mg/g 0.2-12 mg/g 0.2-12 mg/g	-	[78]
Pomelo peel	Tetracycline Oxytetracycline Chlortetracycline	Synthetic swine wastewater	400°C at 10 °C/min, 2 h	80 mg KOH-activated biochar/L, 10 mg/L, pH 7, 21°C, 75 h	2457.4 m^2/g, -, 1.14 cm^3/g	C≡C, C≡N, C-C, C=C, C-H, C-O-C, C=O π-π electron donor–acceptor interaction, electrostatic interaction, pore filling	-	85.0 82.2 96.6	[41]
Corn straw	TS TVSS TC TOC TN NH_4^+-N TP COD K ion Mg ion Cu ion Zn ion Ca ion Fe ion Mn ion	Swine wastewater	500°C, 1 h, N_2 atmosphere	Biochar or NaOH-activated biochar, 10.6 g/L TS, 0.3 g/L TVSS, 2985.6,1908.2, 1270.3, 981.4, 85.7, 4138.6, 655.9, 0.6, 2.7, 1.1, 6.1, 0.5, and 0.2 mg/L for TC, TOC, TV, NH_4^+-N, TP, COD, K, Mg, Cu, Zn, Ca, Fe, and Mn, respectively	-	- H-bonding, electrostatic attraction, ion exchange, hydrophobic interaction	-	50-42 67-67 53-72 55-73 18-33 22-32 19-25 20-26 39-67 33-83 59-41 27-73 30-54 80-80 100	[42]
Platanus balls	Phosphate	Actual wastewater	600°C at 10 °C/min, 2 h, N_2 atmosphere	Column mode, 1 g La-modified biochar	77.01 m^2/g	LaO-, O-PO-, P-O electrostatic adsorption, ligand exchange, complexation	14.85 g/g	-	[63]
Bagasse	Pb ion	Battery manufacturing industry wastewater	300°C, 2.5 h	5 g biochar, pH 5, 2.5 h, 25°C, 2.393 mg/L	12.38 m^2/g	C=O, C=C, C-H, C-N, -COO-, -COOH, -Ph-OH Complexation, ion exchange	12.74 mg/g	75.4	[54]
Potato peel	Cu ion				-	-NH_2	1.117 mg/L	-	

 doi:10.20944/preprints202512.0318.v1

	Pb ion	Industrial wastewater	450°C, 6 L/min of N_2 flow	0.25 g chitosan-modified biochar, 4 h		-	0.506 mg/L		[86]

As listed in Table 4, a variety of agricultural wastes have been used for the adsorption of different contaminants and nutrients from various wastewater. The calcined temperature and duration for biomass carbonization are in the range of 300-900°C and 0.5-6.0 h, respectively, under N_2, Ar, or vacuum atmosphere, depending on the agricultural wastes. The specific surface area, pore diameter, and total pore volume of different pristine biochar range from 1.65 to 428.98 m^2/g, from 1.1 to 20.9 nm, and from 0.0005 to 0.5320 cm^3/g, respectively. The activated biochar usually possesses better porosity and higher surface areas. Functional groups -OH, -COOH, C-H, C=C, and C=O are crucial for the effective adsorption of contaminants from various wastewater. The adsorption equilibrium duration lasts from 40 min to 5 days. It is worth mentioning that due to the abundant diversity of the biochar, contaminations, and the wastewater, making a comparison of the adsorption should be more cautious and difficult.

5. Economic Evaluation and Environmental Impacts

Owing to the high cost-effectiveness, adsorption ability, and large agricultural biomass reserves, biochar has been seen as an excellent alternative adsorbent for activated carbons [46,74]. Accordingly, biochar is ~6-fold cheaper compared to the majority of activated carbons (up to 9 USD/kg) [40]. Compared to activated carbon, the production cost of wheat straw-based biochar is reduced by 34-fold [46]. The energy requirement for preparing biochar was reported to be 15-fold lower compared to activated carbon [46]. Another work states that the cost of biochar (0.08 USD/kg) is 12 times lower than other C-based adsorbents[98]. Specifically, in the Philippines, the evaluated costs are 0.09 USD/kg for plant-based biochar and 1.1-1.7 USD/kg for activated carbons [2]. The costs of biochar prepared from coconut shells [99], pine wood [99], rotten sugarcane bagasse [49], and pomelo peel [41] are 0.8, 0.9, 2.4, and 9.8 USD/kg, respectively. It has been reported that the biochar market share will reach 0.45 billion in US dollars by 2030 globally[58]. Furthermore, the evaluated cost for treating real antibiotic wastewater using biochar is in the range of 9-914 USD/m^3 [12]. For treating livestock wastewater, the cost is expected to be as high as 61.6 thousand USD/year [85]. By using agricultural wastes, optimizing the pyrolysis process for energy efficiency, and ensuring responsible management of the spent biochar, the environmental benefits of wastewater remediation can significantly outweigh the localized or production-related burdens.

The positive environmental impacts of the preparation of biochar using agricultural waste for wastewater remediation are: i) Preventing the decomposition or open burning of agricultural waste minimizes the release of greenhouse gases and other harmful air pollutants; ii) biochar is highly effective at adsorbing and immobilizing a wide range of water contaminants, including heavy metals, nutrients, and recalcitrant organic pollutants, favoring produce cleaner effluent, safeguarding aquatic ecosystems and human health; iii) the pyrolysis process converts the carbon in the agricultural biomass into a highly stable, recalcitrant form C in the biochar, while the used biochar is often co-disposed or applied to soil (where applicable and safe). Around 50% of the original carbon in the biomass feedstock is retained in the stable biochar for centuries, acting as a carbon-negative technology; vi) even though the biochar preparation releases certain waste gases into the atmosphere, the total emission is much decreased compared to the direct incineration, and the good reusability and regeneration properties of biochar reduce the potential environmental impacts [41]. A sustainability assessment described that the preparation of wheat straw-based biochar decreased fossil depletion by 35% and human toxicity by 13% [46]; v) by substituting traditional chemical adsorbents or treatment methods, biochar application can indirectly reduce emissions associated with the production of those alternatives; vi) mitigating the pollution risk of soil induced by agricultural wastes.

Nevertheless, the topic can pose several potential environmental issues, including: i) energy consumption. A study shows that low-temperature slow pyrolysis can be an energetically efficient

 doi:10.20944/preprints202512.0318.v1

strategy, with the energy produced per unit energy input ranging from 2–7 MJ/MJ [100]. The pyrolysis process used to create biochar requires energy (heat), which, if derived from non-renewable sources (*e.g.*, grid electricity or fossil fuels), can contribute to the value of Global Warming Potential and other environmental burdens; ii) gas emissions. It has been reported that the energy consumptions for biochar production were 0.40 and 0.45 kg CO_2(eq) per ton of wood waste during pre-treatment (*e.g.*, chipping and drying) and pyrolysis, respectively. The total for the production process can be up to 0.9.5 kg CO_2(eq) per ton of wood waste [101]. Another work stated that the greenhouse gas emissions (76.6 kg CO_2(eq) per ton) for biochar production were far exceeded by the amount of biochar sequestered long-term (2430 kg CO_2(eq) per ton) [102]. Improper pyrolysis conditions (*e.g.*, low temperature, incomplete combustion) can lead to the release of volatile organic compounds and polycyclic aromatic hydrocarbons, which are environmental and health concerns; iii) precursor transportation. The environmental impact of transporting bulky agricultural waste from its source to the biochar production facility can be significant, influencing overall CO_2 emissions; iv) long-term/post-application Impacts. Although biochar initially immobilizes heavy metals, its aging in the environment can, under certain conditions (*e.g.*, changes in pH or redox potential), lead to the slow release of contaminants back into the environment; v) Contaminants in Biochar. Suppose the agricultural waste itself contains high levels of pollutants (e.g., heavy metals from contaminated soil or feed). In that case, these can become concentrated in the resulting biochar, limiting its safe use for subsequent soil application. These issues can be addressed by valorising the syngas generated during pyrolysis (*e.g.*, to power the process), using higher temperatures and well-controlled systems, locating facilities close to precursor sources, ensuring proper post-treatment disposal, and carefully selecting precursors, respectively. Fortunately, the negative impacts associated with biochar production, such as energy consumption and gas emissions, represent only a minor fraction of the overall life cycle assessment. The process often yields a net environmental benefit owing to carbon sequestration and energy substitution.

6. Future Directions and Challenges

The future perspective of biochar derived from agricultural wastes for wastewater remediation is highly promising, positioning it as a key sustainable technology within the circular economy. This topic converts agricultural residues (a waste management problem) into a value-added adsorbent and provides a cost-effective, eco-friendly alternative to conventional, energy-intensive wastewater treatment methods. The future studies in this field should move beyond simple, pristine biochar to highly engineered, designer materials for specific contaminants and applications. For example, i) the advanced biochar modification to fabricate nanocomposites and the development of innovative biochar (*e.g.*, magnetic biochar) with great reusability, good recyclability, and easy separation from the adsorption systems; ii) the investigation of the fixed bed adsorption and promotion of the biochar's regeneration and recycling properties; iii) the chemical and physical activation utilizing chemical and physical activators to optimize the porosity and surface chemistry for targeted contaminants; iv) Developing 'intelligent' or 'smart' biochar that can adjust their properties (like surface charge) in response to environmental conditions (*e.g.*, pH), allowing for better contaminant retention in dynamic systems; v) Removal of emerging contaminants such as pharmaceuticals, pesticides, and microplastics, where traditional treatments often fall short; vi) recovering valuable resources like nutrients (N and P) and heavy metals from wastewater, turning a pollution problem into a resource opportunity; vii) Synergistic integrating biochar not just as a standalone adsorbent but within hybrid systems, for instance, microbial fuel cells (biochar can serve as an electrode material to enhance electricity generation and pollutant breakdown simultaneously), membrane bioreactors (using biochar as a component in membranes or as a pre-treatment to reduce fouling and improve effluent quality), and algal-biochar systems (utilizing biochar to support microalgae growth for enhanced bioremediation, CO_2 capture, and even biofuel production); viii) estimation of the feasibility of the long-term use of biochar in biofilters; ix) the simultaneous adsorption, decomposition, and mineralization via biodegradation using bacterial-loaded biochar, photocatalysis

 doi:10.20944/preprints202512.0318.v1

or sonocatalysis using biochar as catalysts, and activation of peroxymonosulfate or persulfate for wastewater purification [6,16,24,38,103]; x) optimizing biochar production technologies through innovations in pyrolysis, gasification, and hydrothermal carbonization to improve energy efficiency, enhance scalability, and ensure consistent biochar quality from diverse agricultural feedstocks; xi) Integrating machine learning and Artificial Intelligence with biochar production and application to accurately predict material properties, optimize treatment systems, and manage regeneration/disposal; xii) establishing closed-loop systems where agricultural waste is converted to biochar, used in wastewater treatment, and then the spent biochar (rich in recovered nutrients/carbon) is safely reused as a soil amendment, further supporting sustainable agriculture; and xiii) The scale-up of the obtained lab-outcomes in pilot and industrial levels.

Several challenges should be overcome for scaling up and commercialization: i) Material variability. Establishing standardized protocols for biochar production, characterization, and quality control to ensure consistent performance; ii) Regeneration and disposal. Developing cost-effective and environmentally friendly regeneration methods (e.g., chemical, thermal, biological) for spent biochar to ensure its long-term reusability and prevent secondary pollution; iii) Scalability and cost. Reducing production and modification energy costs to make engineered biochar competitive with established commercial adsorbents like activated carbon on a large scale; iv) Long-term ecotoxicity. Conducting extensive long-term field studies and life cycle assessments to fully understand the environmental stability and potential ecological risks of modified biochar.

7. Conclusions

This review addresses the knowledge gap on the adsorption-based removal of wastewater contaminants using biochar produced from agricultural residues. It compiles the principles of adsorption with agricultural waste-derived biochar, including the general concepts, the interactions between biochar and wastewater contaminants, and schematic descriptions of adsorption processes. It also summarises the preparation, activation, modification, functionalisation, and characterisation of such biochars, and their application to wastewater remediation. In addition, economic assessments, environmental impacts, future directions, and key challenges are presented. Diverse agricultural wastes are valorised to produce biochar that enables efficient decontamination and the recovery of valuable compounds from a range of wastewaters. Most biochar adsorbents show strong performance and reusability in real wastewater treatment. Notably, many studies are titled as investigations of biochar adsorption in wastewater, yet do not actually involve wastewater matrices or treatment scenarios. Further validation and scale-up are essential for the practical implementation of agricultural waste-derived biochar in wastewater remediation.

Author Contributions: Pengyun Liu: Data curation, Writing - Original draft preparation, Investigation, Validation. Luisa Boffa: Investigation, Methodology, Supervision. Giancarlo Cravotto: Conceptualization, Methodology, Supervision, Writing - Reviewing and Editing, *etc.*

Acknowledgments: This research was supported by the University of Turin (Rilo 2024).

Conflicts of Interest: The authors declare no conflicts of interest.

Abbreviations

The following abbreviations are used in this manuscript:

BET	Brunauer–Emmett–Teller
BOD	Biochemical oxygen demand
COD	Chemical oxygen demand
EDS	Energy-dispersive X-ray spectroscopy
FT-IR	Fourier-transform infrared spectroscopy
PFO	Pseudo-first order
pH_L	pH of liquids

 doi:10.20944/preprints202512.0318.v1

pH_{pzc}	Point of zero charge
PSO	Pseudo-second order
SEM	Scanning electron microscopy
TC	Total organic carbon
TDS	Total dissolved solids
TGA	Thermogravimetric Analysis
TOC	Total organic carbon
TS	The total solids
TSS	Total suspended solids
TVSS	Total volatile suspended solids
XPS	X-ray photoelectron spectroscopy
XRD	X-ray diffraction

References

1. Shi, T.-T.; Yang, B.; Hu, W.-G.; Gao, G.-J.; Jiang, X.-Y.; Yu, J.-G. Garlic Peel-Based Biochar Prepared under Weak Carbonation Conditions for Efficient Removal of Methylene Blue from Wastewater. *Molecules* **2024**, *29*, 4772, doi:10.3390/molecules29194772.
2. Alshakhs, F.; Gijjapu, D.R.; Aminul Islam, Md.; Akinpelu, A.A.; Nazal, M.K. A Promising Palm Leaves Waste-Derived Biochar for Efficient Removal of Tetracycline from Wastewater. *J Mol Struct* **2024**, *1296*, 136846, doi:10.1016/j.molstruc.2023.136846.
3. Gao, R.; Ding, S.; Liu, Z.; Jiang, H.; Liu, G.; Fang, J. Recent Advances and Perspectives of Biochar for Livestock Wastewater: Modification Methods, Applications, and Resource Recovery. *J Environ Chem Eng* **2024**, *12*, 113678, doi:10.1016/j.jece.2024.113678.
4. Mihajlović, I.; Hgeig, A.; Novaković, M.; Gvoić, V.; Ubavin, D.; Petrović, M.; Kurniawan, T.A. Valorizing Date Seeds into Biochar for Pesticide Removal: A Sustainable Approach to Agro-Waste-Based Wastewater Treatment. *Sustainability* **2025**, *17*, 5129, doi:10.3390/su17115129.
5. Fan, W.; Zhang, X. Magnetic Coconut Shell Biochar/Sodium Alginate Composite Aerogel Beads for Efficient Removal of Methylene Blue from Wastewater: Synthesis, Characterization, and Mechanism. *Int J Biol Macromol* **2025**, *284*, 137945, doi:10.1016/j.ijbiomac.2024.137945.
6. Wang, Y.; Chen, Y.; Wang, L.; Mo, Y.; Lin, X.; Gao, S.; Chen, M. Efficient Removal of Atrazine in Wastewater by Washed Peanut Shells Biochar: Adsorption Behavior and Biodegradation. *Process Biochemistry* **2025**, *154*, 22–34, doi:10.1016/j.procbio.2025.04.008.
7. Liu, P.; Wu, Z.; Lee, J.; Cravotto, G. Sonocatalytic Degrading Antibiotics over Activated Carbon in Cow Milk. *Food Chem* **2024**, *432*, 137168, doi:10.1016/j.foodchem.2023.137168.
8. Liu, P. Cavitational Technologies for the Removal of Antibiotics in Water and Milk. PhD, University of Turin, 2023.
9. Liu, P.; Wu, Z.; Cannizzo, F.T.; Mantegna, S.; Cravotto, G. Removal of Antibiotics from Milk via Ozonation in a Vortex Reactor. *J Hazard Mater* **2022**, *440*, 129642, doi:10.1016/j.jhazmat.2022.129642.
10. Liu, P.; Wu, Z.; Fang, Z.; Cravotto, G. Sonolytic Degradation Kinetics and Mechanisms of Antibiotics in Water and Cow Milk. *Ultrason Sonochem* **2023**, *99*, 106518, doi:10.1016/j.ultsonch.2023.106518.
11. Ilyas, M.; Liao, Y.; Xu, J.; Wu, S.; Liao, W.; Zhao, X. Removal of Anthracene from Vehicle-Wash Wastewater through Adsorption Using Eucalyptus Wood Waste-Derived Biochar. *Desalination Water Treat* **2024**, *317*, 100115, doi:10.1016/j.dwt.2024.100115.
12. Rizkallah, B.M.; Galal, M.M.; Matta, M.E. Characteristics of Tetracycline Adsorption on Commercial Biochar from Synthetic and Real Wastewater in Batch and Continuous Operations: Study of Removal Mechanisms, Isotherms, Kinetics, Thermodynamics, and Desorption. *Sustainability* **2023**, *15*, 8249, doi:10.3390/su15108249.
13. Yang, Y.; Liu, M.; Tang, S.; You, X.; Li, Y.; Mei, Y.; Chen, Y. Investigation of the Key Mechanisms and Optimum Conditions of High-Effective Phosphate Removal by Bimetallic La-Fe-CNT Film. *Sep Purif Technol* **2024**, *341*, 126938, doi:10.1016/j.seppur.2024.126938.

 doi:10.20944/preprints202512.0318.v1

14. Liu, P.; Wu, Z.; Sun, Z.; Ye, J. Comparison Study of Naphthalene Adsorption on Activated Carbons Prepared from Different Raws. *Korean Journal of Chemical Engineering* **2018**, *35*, 2086–2096, doi:10.1007/s11814-018-0124-7.
15. Liu, P.; Wu, Z.; Ge, X.; Yang, X. Hydrothermal Synthesis and Microwave-Assisted Activation of Starch-Derived Carbons as an Effective Adsorbent for Naphthalene Removal. *RSC Adv* **2019**, *9*, 11696–11706, doi:10.1039/C9RA01386E.
16. Liu, P.; Wu, Z.; Manzoli, M.; Cravotto, G. Magnetic Biochar Generated from Oil-Mill Wastewater by Microwave-Assisted Hydrothermal Treatment for Sonocatalytic Antibiotic Degradation. *J Environ Chem Eng* **2025**, *13*, 114996, doi:10.1016/j.jece.2024.114996.
17. Viotti, P.; Marzeddu, S.; Antonucci, A.; Décima, M.A.; Lovascio, P.; Tatti, F.; Boni, M.R. Biochar as Alternative Material for Heavy Metal Adsorption from Groundwaters: Lab-Scale (Column) Experiment Review. *Materials* **2024**, *17*, 809, doi:10.3390/ma17040809.
18. Boni, M.; Marzeddu, S.; Tatti, F.; Raboni, M.; Mancini, G.; Luciano, A.; Viotti, P. Experimental and Numerical Study of Biochar Fixed Bed Column for the Adsorption of Arsenic from Aqueous Solutions. *Water (Basel)* **2021**, *13*, 915, doi:10.3390/w13070915.
19. Chen, Y.; Cui, Z.; Ding, H.; Wan, Y.; Tang, Z.; Gao, J. Cost-Effective Biochar Produced from Agricultural Residues and Its Application for Preparation of High Performance Form-Stable Phase Change Material via Simple Method. *Int J Mol Sci* **2018**, *19*, 3055, doi:10.3390/ijms19103055.
20. Edwin, T.; Komala, P.S.; Mera, M.; Zulkarnaini, Z.; Jamil, Z. Coconut Shell Biochar as a Sustainable Approach for Nutrient Removal from Agricultural Wastewater. *Journal of Water and Land Development* **2025**, 177–184, doi:10.24425/jwld.2025.154261.
21. Konneh, M.; Wandera, S.M.; Murunga, S.I.; Raude, J.M. Adsorption and Desorption of Nutrients from Abattoir Wastewater: Modelling and Comparison of Rice, Coconut and Coffee Husk Biochar. *Heliyon* **2021**, *7*, doi:10.1016/j.heliyon.2021.e08458.
22. Tariq, M.; Ali Baig, S.; Shams, D.F.; Hussain, S.; Hussain, R.; Qadir, A.; Maryam, H.S.; Khan, Z.U.; Sattar, S.; Xu, X. Dye Wastewater Treatment Using Wheat Straw Biochar in Gadoon Industrial Areas of Swabi, Pakistan. *Water Conservation Science and Engineering* **2022**, *7*, 315–326, doi:10.1007/s41101-022-00144-1.
23. Hossain, N.; Nizamuddin, S.; Griffin, G.; Selvakannan, P.; Mubarak, N.M.; Mahlia, T.M.I. Synthesis and Characterization of Rice Husk Biochar via Hydrothermal Carbonization for Wastewater Treatment and Biofuel Production. *Sci Rep* **2020**, *10*, 18851, doi:10.1038/s41598-020-75936-3.
24. Huong, P.T.; Jitae, K.; Al Tahtamouni, T.M.; Le Minh Tri, N.; Kim, H.-H.; Cho, K.H.; Lee, C. Novel Activation of Peroxymonosulfate by Biochar Derived from Rice Husk toward Oxidation of Organic Contaminants in Wastewater. *Journal of Water Process Engineering* **2020**, *33*, 101037, doi:10.1016/j.jwpe.2019.101037.
25. Pham, T.H.; Chu, T.T.H.; Nguyen, D.K.; Le, T.K.O.; Obaid, S. Al; Alharbi, S.A.; Kim, J.; Nguyen, M.V. Alginate-Modified Biochar Derived from Rice Husk Waste for Improvement Uptake Performance of Lead in Wastewater. *Chemosphere* **2022**, *307*, 135956, doi:10.1016/j.chemosphere.2022.135956.
26. Van Nguyen, Q.; Nguyen, K.M.; Nguyen, H.T.; Duong, T.D.; Dong, M.N.T.; Tran, H.M.T.; Van Hoang, H. Evaluation of Adsorption and Desorption of Wastewater onto Rice Husk Biochar on the Course of Hydroponic Nutrient Production. *Biomass Convers Biorefin* **2025**, *15*, 18615–18628, doi:10.1007/s13399-024-06485-2.
27. Van Nguyen, Q.; Nguyen, K.M.; Nguyen, H.T.; Van Hoang, H.; Duong, T.D.; Dong, M.T.N.; Tran, H.T.M. Transforming Domestic Wastewater into Hydroponic Nutrients Using Corncob-Derived Biochar Adsorption. *J Soil Sci Plant Nutr* **2025**, *25*, 3708–3724, doi:10.1007/s42729-025-02362-7.
28. Hosseini, S.M.; Bojmehrani, A.; Zare, E.; Zare, Z.; Hosseini, S.M.; Bakhshabadi, H. Optimization of Antioxidant Extraction Process from Corn Meal Using Pulsed Electric Field-subcritical Water. *J Food Process Preserv* **2021**, *45*, doi:10.1111/jfpp.15458.
29. Walanda, D.K.; Anshary, A.; Napitupulu, M.; Walanda, R.M. The Utilization of Corn Stalks as Biochar to Adsorb BOD and COD in Hospital Wastewater. *International Journal of Design and Nature and Ecodynamics* **2022**, *17*, 113–118, doi:10.18280/ijdne.170114.

 doi:10.20944/preprints202512.0318.v1

30. Lou, L.; Li, W.; Yao, H.; Luo, H.; Liu, G.; Fang, J. Corn Stover Waste Preparation Cerium-Modified Biochar for Phosphate Removal from Pig Farm Wastewater: Adsorption Performance and Mechanism. *Biochem Eng J* **2024**, *212*, 109530, doi:10.1016/j.bej.2024.109530.
31. Chu, T.T.H.; Nguyen, M.V. Improved Cr (VI) Adsorption Performance in Wastewater and Groundwater by Synthesized Magnetic Adsorbent Derived from Fe_3O_4 Loaded Corn Straw Biochar. *Environ Res* **2023**, *216*, 114764, doi:10.1016/j.envres.2022.114764.
32. Favre, F.; Slijepcevic, A.; Piantini, U.; Frey, U.; Abiven, S.; Schmidt, H.-P.; Charlet, L. Real Wastewater Micropollutant Removal by Wood Waste Biomass Biochars: A Mechanistic Interpretation Related to Various Biochar Physico-Chemical Properties. *Bioresour Technol Rep* **2022**, *17*, 100966, doi:10.1016/j.biteb.2022.100966.
33. Chen, H.; Guo, H.; Jiang, D.; Cheng, S.; Xing, B.; Meng, W.; Fang, J.; Xia, H. Microwave-Assisted Pyrolysis of Rape Stalk to Prepare Biochar for Heavy Metal Wastewater Removal. *Diam Relat Mater* **2023**, *134*, 109794, doi:10.1016/j.diamond.2023.109794.
34. Wainaina, S.; Awasthi, M.K.; Sarsaiya, S.; Chen, H.; Singh, E.; Kumar, A.; Ravindran, B.; Awasthi, S.K.; Liu, T.; Duan, Y.; et al. Resource Recovery and Circular Economy from Organic Solid Waste Using Aerobic and Anaerobic Digestion Technologies. *Bioresour Technol* **2020**, *301*, 122778, doi:10.1016/j.biortech.2020.122778.
35. Das, S.K.; Ghosh, G.K.; Avasthe, R. Conversion of Crop, Weed and Tree Biomass into Biochar for Heavy Metal Removal and Wastewater Treatment. *Biomass Convers Biorefin* **2023**, *13*, 4901–4914, doi:10.1007/s13399-021-01334-y.
36. Liu, P.; Wu, Z.; Barge, A.; Boffa, L.; Martina, K.; Cravotto, G. Determination of Trace Antibiotics in Water and Milk via Preconcentration and Cleanup Using Activated Carbons. *Food Chem* **2022**, *385*, 132695, doi:10.1016/j.foodchem.2022.132695.
37. Masmoudi, M.A.; Abid, N.; Feki, F.; Karray, F.; Chamkha, M.; Sayadi, S. Study of Olive Mill Wastewater Adsorption onto Biochar as a Pretreatment Option within a Fully Integrated Process. *EuroMediterr J Environ Integr* **2024**, *9*, 621–635, doi:10.1007/s41207-024-00464-9.
38. Fito, J.; Abewaa, M.; Nkambule, T. Magnetite-Impregnated Biochar of Parthenium Hysterophorus for Adsorption of Cr(VI) from Tannery Industrial Wastewater. *Appl Water Sci* **2023**, *13*, 78, doi:10.1007/s13201-023-01880-y.
39. Abdu, M.; Babaee, S.; Worku, A.; Msagati, T.A.M.; Nure, J.F. The Development of Giant Reed Biochar for Adsorption of Basic Blue 41 and Eriochrome Black T. Azo Dyes from Wastewater. *Sci Rep* **2024**, *14*, 18320, doi:10.1038/s41598-024-67997-5.
40. Collivignarelli, M.C.; Illankoon, W.A.M.A.N.; Milanese, C.; Calatroni, S.; Caccamo, F.M.; Medina-Llamas, M.; Girella, A.; Sorlini, S. Preparation and Modification of Biochar Derived from Agricultural Waste for Metal Adsorption from Urban Wastewater. *Water (Basel)* **2024**, *16*, 698, doi:10.3390/w16050698.
41. Cheng, D.; Ngo, H.H.; Guo, W.; Chang, S.W.; Nguyen, D.D.; Zhang, X.; Varjani, S.; Liu, Y. Feasibility Study on a New Pomelo Peel Derived Biochar for Tetracycline Antibiotics Removal in Swine Wastewater. *Science of The Total Environment* **2020**, *720*, 137662, doi:10.1016/j.scitotenv.2020.137662.
42. Yu, J.; Hu, H.; Wu, X.; Zhou, T.; Liu, Y.; Ruan, R.; Zheng, H. Coupling of Biochar-Mediated Absorption and Algal-Bacterial System to Enhance Nutrients Recovery from Swine Wastewater. *Science of The Total Environment* **2020**, *701*, 134935, doi:10.1016/j.scitotenv.2019.134935.
43. Díaz, B.; Sommer-Márquez, A.; Ordoñez, P.E.; Bastardo-González, E.; Ricaurte, M.; Navas-Cárdenas, C. Synthesis Methods, Properties, and Modifications of Biochar-Based Materials for Wastewater Treatment: A Review. *Resources* **2024**, *13*, 8, doi:10.3390/resources13010008.
44. Idris, M.O.; Yaqoob, A.A.; Ibrahim, M.N.M.; Ahmad, A.; Alshammari, M.B. Introduction of Adsorption Techniques for Heavy Metals Remediation. In *Emerging Techniques for Treatment of Toxic Metals from Wastewater*; Elsevier, 2023; pp. 1–18.
45. Wu, Z.; Sun, Z.; Liu, P.; Li, Q.; Yang, R.; Yang, X. Competitive Adsorption of Naphthalene and Phenanthrene on Walnut Shell Based Activated Carbon and the Verification *via* Theoretical Calculation. *RSC Adv* **2020**, *10*, 10703–10714, doi:10.1039/C9RA09447D.

 doi:10.20944/preprints202512.0318.v1

46. Yu, Y.; Yang, B.; Petropoulos, E.; Duan, J.; Yang, L.; Xue, L. The Potential of Biochar as N Carrier to Recover N from Wastewater for Reuse in Planting Soil: Adsorption Capacity and Bioavailability Analysis. *Separations* **2022**, *9*, 337, doi:10.3390/separations9110337.
47. Wu, Z.; Liu, P.; Wu, Z.; Cravotto, G. In Situ Modification of Activated Carbons by Oleic Acid under Microwave Heating to Improve Adsorptive Removal of Naphthalene in Aqueous Solutions. *Processes* **2021**, *9*, 391, doi:10.3390/pr9020391.
48. Yusuff, A.S.; Popoola, L.T.; Ibrahim, I.S. Adsorptive Removal of Anthraquinone Dye from Wastewater Using Silica-Nitrogen Reformed Eucalyptus Bark Biochar: Parametric Optimization, Isotherm and Kinetic Studies. *J Taiwan Inst Chem Eng* **2025**, *166*, 105503, doi:10.1016/j.jtice.2024.105503.
49. Bai, X.; Zhang, M.; Niu, B.; Zhang, W.; Wang, X.; Wang, J.; Wu, D.; Wang, L.; Jiang, K. Rotten Sugarcane Bagasse Derived Biochars with Rich Mineral Residues for Effective Pb (II) Removal in Wastewater and the Tech-Economic Analysis. *J Taiwan Inst Chem Eng* **2022**, *132*, 104231, doi:10.1016/j.jtice.2022.104231.
50. Wang, G.; Yang, R.; Liu, Y.; Wang, J.; Tan, W.; Liu, X.; Jin, Y.; Qu, J. Adsorption of Cd(II) onto Auricularia Auricula Spent Substrate Biochar Modified by CS_2: Characteristics, Mechanism and Application in Wastewater Treatment. *J Clean Prod* **2022**, *367*, 132882, doi:10.1016/j.jclepro.2022.132882.
51. Enaime, G.; Baçaoui, A.; Yaacoubi, A.; Lübken, M. Biochar for Wastewater Treatment—Conversion Technologies and Applications. *Applied Sciences* **2020**, *10*, 3492, doi:10.3390/app10103492.
52. Adewoye, T.L.; Ogunleye, O.O.; Abdulkareem, A.S.; Salawudeen, T.O.; Tijani, J.O. Optimization of the Adsorption of Total Organic Carbon from Produced Water Using Functionalized Multi-Walled Carbon Nanotubes. *Heliyon* **2021**, *7*, e05866, doi:10.1016/j.heliyon.2020.e05866.
53. Ghebrehiwot, H.; Fynn, R.; Morris, C.; Kirkman, K. Shoot and Root Biomass Allocation and Competitive Hierarchies of Four South African Grass Species on Light, Soil Resources and Cutting Gradients. *Afr J Range Forage Sci* **2006**, *23*, 113–122, doi:10.2989/10220110609485894.
54. Poonam; Bharti, S.K.; Kumar, N. Kinetic Study of Lead (Pb^{2+}) Removal from Battery Manufacturing Wastewater Using Bagasse Biochar as Biosorbent. *Appl Water Sci* **2018**, *8*, 119, doi:10.1007/s13201-018-0765-z.
55. Ashebir, H.; Nure, J.F.; Worku, A.; Msagati, T.A.M. Prosopis Juliflora Biochar for Adsorption of Sulfamethoxazole and Ciprofloxacin from Pharmaceutical Wastewater. *Desalination Water Treat* **2024**, *320*, doi:10.1016/j.dwt.2024.100691.
56. Tang, G.; Mo, H.; Gao, L.; Chen, Y.; Zhou, X. Adsorption of Crystal Violet from Wastewater Using Alkaline-Modified Pomelo Peel-Derived Biochar. *Journal of Water Process Engineering* **2024**, *68*, 106334, doi:10.1016/j.jwpe.2024.106334.
57. Cui, Y.; Du, W.; Zhang, Y.; Hu, J.; Kang, W. Adsorption Characteristics and Removal Mechanism of Quinoline in Wastewater by Walnut Shell-Based Biochar. *Journal of Water Process Engineering* **2025**, *70*, 106980, doi:10.1016/j.jwpe.2025.106980.
58. Ou, W.; Lan, X.; Guo, J.; Cai, A.; Liu, P.; Liu, N.; Liu, Y.; Lei, Y. Preparation of Iron/Calcium-Modified Biochar for Phosphate Removal from Industrial Wastewater. *J Clean Prod* **2023**, *383*, 135468, doi:10.1016/j.jclepro.2022.135468.
59. Illankoon, W.A.M.A.N.; Milanese, C.; Karunarathna, A.K.; Liyanage, K.D.H.E.; Alahakoon, A.M.Y.W.; Rathnasiri, P.G.; Collivignarelli, M.C.; Sorlini, S. Evaluating Sustainable Options for Valorization of Rice By-Products in Sri Lanka: An Approach for a Circular Business Model. *Agronomy* **2023**, *13*, 803, doi:10.3390/agronomy13030803.
60. Jeyasubramanian, K.; Thangagiri, B.; Sakthivel, A.; Dhaveethu Raja, J.; Seenivasan, S.; Vallinayagam, P.; Madhavan, D.; Malathi Devi, S.; Rathika, B. A Complete Review on Biochar: Production, Property, Multifaceted Applications, Interaction Mechanism and Computational Approach. *Fuel* **2021**, *292*, 120243, doi:10.1016/j.fuel.2021.120243.
61. Ambaye, T.G.; Vaccari, M.; van Hullebusch, E.D.; Amrane, A.; Rtimi, S. Mechanisms and Adsorption Capacities of Biochar for the Removal of Organic and Inorganic Pollutants from Industrial Wastewater. *International Journal of Environmental Science and Technology* **2021**, *18*, 3273–3294, doi:10.1007/s13762-020-03060-w.

 doi:10.20944/preprints202512.0318.v1

62. Kılıç, M.; Keskin, M.E.; Mazlum, S.; Mazlum, N. Hg(II) and Pb(II) Adsorption on Activated Sludge Biomass: Effective Biosorption Mechanism. *Int J Miner Process* **2008**, *87*, 1–8, doi:10.1016/j.minpro.2008.01.001.
63. Jia, Z.; Zeng, W.; Xu, H.; Li, S.; Peng, Y. Adsorption Removal and Reuse of Phosphate from Wastewater Using a Novel Adsorbent of Lanthanum-Modified Platanus Biochar. *Process Safety and Environmental Protection* **2020**, *140*, 221–232, doi:10.1016/j.psep.2020.05.017.
64. Xiao, X.; Chen, B.; Chen, Z.; Zhu, L.; Schnoor, J.L. Insight into Multiple and Multilevel Structures of Biochars and Their Potential Environmental Applications: A Critical Review. *Environ Sci Technol* **2018**, *52*, 5027–5047, doi:10.1021/acs.est.7b06487.
65. Wu, Z.; Liu, P.; Wu, Z.; Cravotto, G. In Situ Modification of Activated Carbons by Oleic Acid under Microwave Heating to Improve Adsorptive Removal of Naphthalene in Aqueous Solutions. *Processes* **2021**, *9*, 391, doi:10.3390/pr9020391.
66. Tan, K.L.; Hameed, B.H. Insight into the Adsorption Kinetics Models for the Removal of Contaminants from Aqueous Solutions. *J Taiwan Inst Chem Eng* **2017**, *74*, 25–48, doi:10.1016/j.jtice.2017.01.024.
67. Musah, M.; Azeh, Y.; Mathew, J.; Umar, M.; Abdulhamid, Z.; Muhammad, A. Adsorption Kinetics and Isotherm Models: A Review. *Caliphate Journal of Science and Technology* **2022**, *4*, 20–26, doi:10.4314/cajost.v4i1.3.
68. Wang, Y.; Wang, C.; Huang, X.; Zhang, Q.; Wang, T.; Guo, X. Guideline for Modeling Solid-Liquid Adsorption: Kinetics, Isotherm, Fixed Bed, and Thermodynamics. *Chemosphere* **2024**, *349*, 140736, doi:10.1016/j.chemosphere.2023.140736.
69. Al-Ghouti, M.A.; Da'ana, D.A. Guidelines for the Use and Interpretation of Adsorption Isotherm Models: A Review. *J Hazard Mater* **2020**, *393*, 122383, doi:10.1016/j.jhazmat.2020.122383.
70. Largitte, L.; Pasquier, R. A Review of the Kinetics Adsorption Models and Their Application to the Adsorption of Lead by an Activated Carbon. *Chemical Engineering Research and Design* **2016**, *109*, 495–504, doi:10.1016/j.cherd.2016.02.006.
71. Yang, Y.; You, X.; Tang, S.; Li, Y.; Liu, M.; Mei, Y.; Shu, W. Phosphate Uptake over the Innovative La–Fe–CNT Membrane: Structure-Activity Correlation and Mechanism Investigation. *ACS ES&T Engineering* **2024**, *4*, 2642–2656, doi:10.1021/acsestengg.4c00321.
72. Soundari, L.; Prasanna, K. Optimum Usage of Biochar Derived from Agricultural Biomass in Removing Organic Pollutant Present in Pharmaceutical Wastewater. *Sustainable Chemistry for the Environment* **2025**, *10*, 100259, doi:10.1016/j.scenv.2025.100259.
73. Freundlich, H. Über Die Adsorption in Lösungen. *Zeitschrift für Physikalische Chemie* **1907**, *57U*, 385–470, doi:10.1515/zpch-1907-5723.
74. Fseha, Y.H.; Shaheen, J.; Sizirici, B. Phenol Contaminated Municipal Wastewater Treatment Using Date Palm Frond Biochar: Optimization Using Response Surface Methodology. *Emerg Contam* **2023**, *9*, 100202, doi:10.1016/j.emcon.2022.100202.
75. Zhao, X.; Wang, Q.; Sun, Y.; Li, H.; Lei, Z.; Zheng, B.; Xia, H.; Su, Y.; Ali, K.M.Y.; Wang, H.; et al. Beryllium Adsorption from Beryllium Mining Wastewater with Novel Porous Lotus Leaf Biochar Modified with PO_4^{3-}/NH_4^+ Multifunctional Groups (MLLB). *Biochar* **2024**, *6*, 89, doi:10.1007/s42773-024-00385-4.
76. Amdeha, E. Biochar-Based Nanocomposites for Industrial Wastewater Treatment via Adsorption and Photocatalytic Degradation and the Parameters Affecting These Processes. *Biomass Convers Biorefin* 2024, *14*, 23293–23318.
77. Motasemi, F.; Afzal, M.T. A Review on the Microwave-Assisted Pyrolysis Technique. *Renewable and Sustainable Energy Reviews* **2013**, *28*, 317–330, doi:10.1016/j.rser.2013.08.008.
78. Gayathri, R.; Gopinath, K.P.; Kumar, P.S. Adsorptive Separation of Toxic Metals from Aquatic Environment Using Agro Waste Biochar: Application in Electroplating Industrial Wastewater. *Chemosphere* **2021**, *262*, 128031, doi:10.1016/j.chemosphere.2020.128031.
79. Sutarut, P.; Cheirsilp, B.; Boonsawang, P. The Potential of Oil Palm Frond Biochar for the Adsorption of Residual Pollutants from Real Latex Industrial Wastewater. *Int J Environ Res* **2023**, *17*, 16, doi:10.1007/s41742-022-00503-9.
80. Liu, W.-J.; Jiang, H.; Yu, H.-Q. Development of Biochar-Based Functional Materials: Toward a Sustainable Platform Carbon Material. *Chem Rev* **2015**, *115*, 12251–12285, doi:10.1021/acs.chemrev.5b00195.

 doi:10.20944/preprints202512.0318.v1

81. Yap, M.W.; Mubarak, N.M.; Sahu, J.N.; Abdullah, E.C. Microwave Induced Synthesis of Magnetic Biochar from Agricultural Biomass for Removal of Lead and Cadmium from Wastewater. *Journal of Industrial and Engineering Chemistry* **2017**, *45*, 287–295, doi:10.1016/j.jiec.2016.09.036.
82. Hassan, N.S.; Jalil, A.A.; Izzuddin, N.M.; Bahari, M.B.; Hatta, A.H.; Kasmani, R.M.; Norazahar, N. Recent Advances in Lignocellulosic Biomass-Derived Biochar-Based Photocatalyst for Wastewater Remediation. *J Taiwan Inst Chem Eng* **2024**, *163*, 105670, doi:10.1016/j.jtice.2024.105670.
83. Gao, L.; Goldfarb, J.L. Heterogeneous Biochars from Agriculture Residues and Coal Fly Ash for the Removal of Heavy Metals from Coking Wastewater. *RSC Adv* **2019**, *9*, 16018–16027, doi:10.1039/C9RA02459J.
84. Vu, N.-T.; Do, K.-U. Insights into Adsorption of Ammonium by Biochar Derived from Low Temperature Pyrolysis of Coffee Husk. *Biomass Convers Biorefin* **2023**, *13*, 2193–2205, doi:10.1007/s13399-021-01337-9.
85. Lap, B.Q.; Thinh, N.V.D.; Hung, N.T.Q.; Nam, N.H.; Dang, H.T.T.; Ba, H.T.; Ky, N.M.; Tuan, H.N.A. Assessment of Rice Straw–Derived Biochar for Livestock Wastewater Treatment. *Water Air Soil Pollut* **2021**, *232*, 162, doi:10.1007/s11270-021-05100-8.
86. Hussain, A.; Maitra, J.; Khan, K.A. Development of Biochar and Chitosan Blend for Heavy Metals Uptake from Synthetic and Industrial Wastewater. *Appl Water Sci* **2017**, *7*, 4525–4537, doi:10.1007/s13201-017-0604-7.
87. Lee, J.W.; Han, J.; Choi, Y.-K.; Park, S.; Lee, S.H. Reswellable Alginate/Activated Carbon/Carboxymethyl Cellulose Hydrogel Beads for Ibuprofen Adsorption from Aqueous Solutions. *Int J Biol Macromol* **2023**, *249*, 126053, doi:10.1016/j.ijbiomac.2023.126053.
88. Qiu, L.; Zheng, P.; Zhang, M.; Yu, X.; Abbas, G. Phosphorus Removal Using Ferric–Calcium Complex as Precipitant: Parameters Optimization and Phosphorus-Recycling Potential. *Chemical Engineering Journal* **2015**, *268*, 230–235, doi:10.1016/j.cej.2014.12.107.
89. Kumi, A.G.; Ibrahim, M.G.; Fujii, M.; Nasr, M. Petrochemical Wastewater Treatment by Eggshell Modified Biochar as Adsorbent: Atechno-Economic and Sustainable Approach. *Adsorption Science & Technology* **2022**, *2022*, doi:10.1155/2022/2323836.
90. Zhang, P.; Duan, W.; Peng, H.; Pan, B.; Xing, B. Functional Biochar and Its Balanced Design. *ACS Environmental Au* **2022**, *2*, 115–127, doi:10.1021/acsenvironau.1c00032.
91. Muzyka, R.; Misztal, E.; Hrabak, J.; Banks, S.W.; Sajdak, M. Various Biomass Pyrolysis Conditions Influence the Porosity and Pore Size Distribution of Biochar. *Energy* **2023**, *263*, 126128, doi:10.1016/j.energy.2022.126128.
92. Thommes, M.; Kaneko, K.; Neimark, A. V.; Olivier, J.P.; Rodriguez-Reinoso, F.; Rouquerol, J.; Sing, K.S.W. Physisorption of Gases, with Special Reference to the Evaluation of Surface Area and Pore Size Distribution (IUPAC Technical Report). *Pure and Applied Chemistry* **2015**, *87*, 1051–1069, doi:10.1515/pac-2014-1117.
93. Ezeonuegbu, B.A.; Machido, D.A.; Whong, C.M.Z.; Japhet, W.S.; Alexiou, A.; Elazab, S.T.; Qusty, N.; Yaro, C.A.; Batiha, G.E.-S. Agricultural Waste of Sugarcane Bagasse as Efficient Adsorbent for Lead and Nickel Removal from Untreated Wastewater: Biosorption, Equilibrium Isotherms, Kinetics and Desorption Studies. *Biotechnology Reports* **2021**, *30*, e00614, doi:10.1016/j.btre.2021.e00614.
94. Shruthi, S.; Vishalakshi, B. Hybrid Banana Pseudo Stem Biochar- Poly (N-Hydroxyethylacrylamide) Hydrogel and Its Magnetic Nanocomposite for Effective Remediation of Dye from Wastewater. *J Environ Chem Eng* **2024**, *12*, 112682, doi:10.1016/j.jece.2024.112682.
95. Egila, J.N.; Dauda, B.E.N.; Iyaka, Y.A.; Jimoh, T. Agricultural Waste as a Low Cost Adsorbent for Heavy Metal Removal from Wastewater. *Int J Phys Sci* **2011**, *6*, 2152–2157.
96. El Ouassif, H.; Gayh, U.; Ghomi, M.R. Biochar Production from Agricultural Waste (Corncob) to Remove Ammonia from Livestock Wastewater. *International Journal of Recycling of Organic Waste in Agriculture* **2024**, *13*, doi:10.57647/j.ijrowa.2024.1301.09.
97. Choudhary, V.; Philip, L. Sustainability Assessment of Acid-Modified Biochar as Adsorbent for the Removal of Pharmaceuticals and Personal Care Products from Secondary Treated Wastewater. *J Environ Chem Eng* **2022**, *10*, 107592, doi:10.1016/j.jece.2022.107592.
98. Yoder, J.; Galinato, S.; Granatstein, D.; Garcia-Pérez, M. Economic Tradeoff between Biochar and Bio-Oil Production via Pyrolysis. *Biomass Bioenergy* **2011**, *35*, 1851–1862, doi:10.1016/j.biombioe.2011.01.026.

 doi:10.20944/preprints202512.0318.v1

99. Fdez-Sanromán, A.; Pazos, M.; Rosales, E.; Sanromán, M.A. Unravelling the Environmental Application of Biochar as Low-Cost Biosorbent: A Review. *Applied Sciences* **2020**, *10*, 7810, doi:10.3390/app10217810.
100. Gaunt, J.L.; Lehmann, J. Energy Balance and Emissions Associated with Biochar Sequestration and Pyrolysis Bioenergy Production. *Environ Sci Technol* **2008**, *42*, 4152–4158, doi:10.1021/es071361i.
101. An, J.Y.; Hwang, G.Y.; Um, J.B. An Analysis of the Influence Factors of Farmers' Acceptance Intention on Low Carbon Agricultural Technology Bio-Char. *Journal of Agricultural Extension & Community Development* **2023**, *30*, 199–212.
102. Bergman, R.D.; Zhang, * -Hanwen; Englund, K.; Windell, K.; Gu, H. *Curitiba, Brazil Proceedings of the 59th International Convention of Society of Wood Science and Technology*; 2016;
103. Thuan, D. Van; Chu, T.T.H.; Thanh, H.D.T.; Le, M.V.; Ngo, H.L.; Le, C.L.; Thi, H.P. Adsorption and Photodegradation of Micropollutant in Wastewater by Photocatalyst TiO_2/Rice Husk Biochar. *Environ Res* **2023**, *236*, 116789, doi:10.1016/j.envres.2023.116789.